

Stretchable Energy Storage Devices Based on Carbon Materials

Luhe Li, Lie Wang, Tingting Ye, Huisheng Peng,* and Ye Zhang*

Stretchable energy storage devices are essential for developing stretchable electronics and have thus attracted extensive attention in a variety of fields including wearable devices and bioelectronics. Carbon materials, e.g., carbon nanotube and graphene, are widely investigated as electrode materials for energy storage devices due to their large specific surface areas and combined remarkable electrical and electrochemical properties. They can also be effectively composited with many other functional materials or designed into different microstructures for fabricating stretchable energy storage devices. This review summarizes recent advances toward the development of carbon-material-based stretchable energy storage devices. An overview of common carbon materials' fundamental properties and general strategies to enable the stretchability of carbon-material-based electrodes are presented. The performances of the as-fabricated stretchable energy storage devices including supercapacitors, lithium-ion batteries, metal–air batteries, and other batteries are then carefully discussed. Challenges and perspectives in this emerging field are finally highlighted for future studies.

reliable working, and comfortable wearing experience.^[8–10] For efficiently powering these stretchable electronic devices, stretchable energy storage devices that perform approximative mechanical elastic property with the electronic devices while maintaining high electrochemical performance are highly desired.^[11–13]

Supercapacitors and lithium-ion (Li-ion) batteries are two kinds of the most studied energy storage devices.^[14] Supercapacitors are widely explored for high power densities with promising advantages of easy fabrication, electrochemical stability, and long-term durability.^[15] While, Li-ion batteries have been mainly investigated for higher energy densities to achieve continuous and stable power functions.^[16] Besides, metal–air batteries (Li–air, Zn–air, and Al–air batteries) with high theoretical energy densities and other batteries (Na-ion, K-ion, and Zn-ion batteries)

with high safety have also emerged as promising candidates for next-generation energy storage devices.^[17–19] Numerous efforts have recently been devoted to making these devices stretchable. Generally, the properties of stretchable energy storage devices are mainly evaluated by the stretchability and electrochemical performances. They are typically required to have stretchability of >100% and meanwhile without prejudice to the electrochemical properties (e.g., energy density, power density, and cycling performance) to meet the wearable applications.

Developing a stretchable electrode is the key to achieve a high-performance stretchable energy storage device. Presently, metals, metal oxides, inorganic compounds, conductive polymers, and carbon materials are mainly used as electrode materials for energy storage devices. Among them, carbon materials are demonstrated for excellent comprehensive properties and have been thus widely used to construct stretchable electrodes for the following reasons (**Figure 1**). 1) Carbon materials, such as carbon nanotube (CNT) and graphene, have large specific surface areas, remarkable electrical and electrochemical properties, which satisfy the demands of working as electrode materials. 2) Compared with other materials, the properties of carbon materials can be easily adjusted in the production process or by various post-treatment methods. They can be uniformly mixed with elastic polymer materials to form stretchable composite electrodes. 3) Carbon materials usually perform high mechanical strength, good flexibility, and superior processability. Thus, they can be easily manufactured into various stretchable structures such

1. Introduction

Wearable electronic devices have experienced a booming development in the past decade, mainly attributed to the advances in semiconductor fabrication technology, sensing technology, and material manufacturing processes.^[1–4] These innovations not only enable wearable devices with a smaller size, lower power consumption but also make the concepts of real-time health monitoring and closed-loop treatment come true.^[5–7] To meet the demands of various wearable applications, wearable electronic devices are required to be stretchable for providing stable interfaces with the human body for high-accuracy sensing,

L. Li, Dr. L. Wang, T. Ye, Prof. Y. Zhang
National Laboratory of Solid State Microstructures
Jiangsu Key Laboratory of Artificial Functional Materials
College of Engineering and Applied Sciences
Nanjing University
Nanjing 210023, China
E-mail: yezhang@nju.edu.cn

Dr. L. Wang, Prof. H. Peng
State Key Laboratory of Molecular Engineering of Polymers
Department of Macromolecular Science and Laboratory
of Advanced Materials
Fudan University
Shanghai 200438, China
E-mail: penghs@fudan.edu.cn

 The ORCID identification number(s) for the author(s) of this article can be found under <https://doi.org/10.1002/smll.202005015>.

DOI: 10.1002/smll.202005015

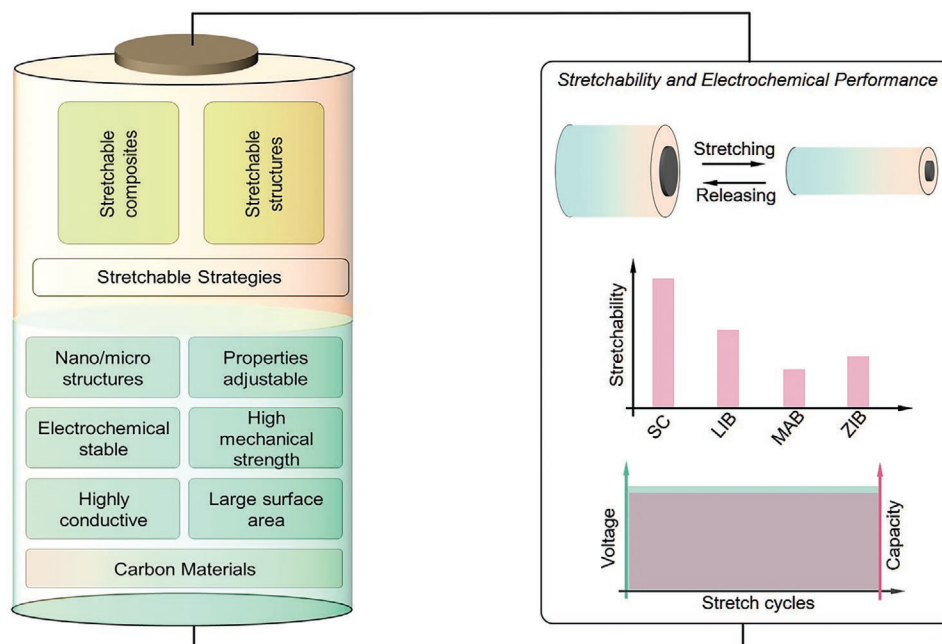


Figure 1. Schematic illustration to show the merits of carbon materials for fabricating stretchable energy storage devices. SC: supercapacitor, LIB: Li-ion battery, MAB: metal–air battery, ZIB: Zn-ion battery.

as wavy, kirigami-patterned, and spring-like architectures to achieve stretchability.

Although several reviews have reported the late progress of stretchable energy storage devices, few of them focus on the widely used carbon materials.^[16,20,21] Meanwhile, some reviews summarized the role of carbon materials in the field of stretchable supercapacitors, it is rare to discuss carbon materials for Li-ion batteries, metal–air batteries, and some other batteries.^[22,23] Herein, we present a timely and comprehensive review of stretchable energy storage devices based on carbon materials to highlight the significance of carbon materials in this specific field. First, the basic properties of common carbon materials are introduced. An overview of general strategies to fabricate stretchable carbon-material-based electrodes is described from two aspects of compositing with elastomer and designing stretchable structures. Subsequently, stretchable carbon-based supercapacitors, Li-ion batteries, metal–air batteries, and other batteries are summarized to focus on their electrochemical properties and mechanical stretchability. Finally, the remaining challenges and future opportunities for this emerging field are discussed.

2. Carbon Materials for Energy Storage Devices

2.1. Graphene

Graphene is a 2D single-layer carbon sheet with a hexagonal packed lattice structure. It owns many unique properties, such as a large theoretical specific surface area of $2630 \text{ m}^2 \text{ g}^{-1}$, the high carrier mobility of about $10\,000 \text{ cm}^2 \text{ V}^{-1} \text{ s}^{-1}$ at room temperature, which are favorable for energy storage devices.^[24] The specific capacitance of single-layer-graphene-electrode-based

supercapacitor was measured to be $\approx 21 \mu\text{F cm}^{-2}$ and the theoretical capacitance will be $\approx 550 \text{ F g}^{-1}$ if the surface area of the graphene can be fully used.^[25]

Chemical vapor deposition is the most used method to synthesize a single-layered graphene sheet. The fabricated graphene sheet is flexible, transparent ($\approx 97.4\%$), and electrically conductive (hundreds of $\Omega \text{ sq}^{-1}$).^[26,27] However, the low yield and high cost of chemical vapor deposition severely limit the application. Reducing graphene oxide into graphene is another common method to produce graphene powders.^[28] In this approach, graphite powder is first oxidized into graphite oxide by a strong oxidizer (e.g., H_2SO_4 and KMnO_4). In this approach, oxygen functional groups are inserted between two neighboring graphite layers to reduce van der Waals force for easier detaching. External forces detach the single-layered or multilayered graphene oxide (e.g., ultrasonication and high temperature). Subsequently, the graphene oxide is reduced into graphene. Compared to the chemical vapor deposition method, reducing graphene oxide into graphene has the advantages of easier operation, lower cost, and higher yield. The obtained graphene powders are usually used as conductive fillers to increase the conductivity of the electrodes.

Graphene can be easily assembled into different forms, including paper, foam, and fiber for energy storage devices.^[29–31] Graphene papers have attracted much attention due to being thickness tunable, lightweight, flexible, and electrically conductive.^[32] Continuous efforts have been devoted to exploring fabrication methods, including spin coating, layer-by-layer deposition, vacuum filtration, and interfacial assembly.^[33–37] Note that graphene tends to agglomerate and restack together due to π – π interaction and van der Waals force, which will decrease the specific surface areas and limit the diffusion of electron ions among graphene layers.^[38] Using appropriate spacers, such as carbon blacks, CNTs, and metal particles, can effectively overcome this

challenge.^[39–42] For example, a flexible graphene paper electrode with carbon black as a spacer showed an open structure for charge storage and ion diffusion, resulting in a significant improvement in electrochemical performance.^[39]

Fabricating graphene into a 3D porous foam by using nickel foam as a catalyst can significantly increase the capability to form composite materials with other phases.^[43,44] The plenty of void spaces are suitable for loading abundant active materials and providing a large specific surface area, which are welcomed for energy storage devices. Moreover, attributed to the interconnected networks, graphene foam can maintain its high conductivity even at a relatively high strain, making it suitable for working as stretchable electrodes.

In addition to graphene paper and graphene foam, graphene fiber also plays a critical role in constructing fiber energy storage devices for powering wearable electronic devices. A graphene fiber can be obtained by continuous wet spinning of graphene oxide suspension followed by a chemical/thermal reduction to rebuild the graphene lattice.^[45] The mechanical and electrical properties of graphene fiber can be easily adjusted by controlling the treatment temperature, the suspension's microstructure, and the spinning procedures. For example, by controlling the orientation of graphene fiber and the concentration of spinning dope and using high-temperature post-treatment, researchers have synthesized a flexible kilometer-scale continuous graphene fiber simultaneously with superior mechanical (high modulus of 400 GPa) and electrical properties (electrical conductivity of $8 \times 10^5 \text{ S m}^{-1}$).^[46]

2.2. Carbon Nanotube

CNTs can be briefly divided into single-walled, double-walled, and multiwalled CNTs. Single-walled CNT (SWCNT) can be considered as a cylindrical tube formed by the wrapping of a single-layered graphene sheet, while multiwalled CNT (MWCNT) is a central tubule with nanometric diameter surrounded by graphitic layers separated by $\approx 0.34 \text{ nm}$, and its diameter is typically ranged from 10 to 20 nm.^[47] Attributed to its unusual structure, CNT performed a high electrical conductivity of 10^5 S cm^{-1} and a large specific surface area.^[48] Due to these fundamental merits, CNTs have been widely used as conductive additives or made into a 3D conductive network to improve the electrochemical kinetics of active materials, which promote electron transports and ion diffusions for high rate performances.^[49] Besides, the theoretical specific capacity of commercial graphite anode for Li-ion batteries is 372 mAh g^{-1} , while it can be improved to over 1000 mAh g^{-1} when single-walled CNTs were introduced as the anode because of the formation of Li_xC and the intercalation of Li ion into CNTs.^[50,51] Moreover, the high mechanical strength and high aspect ratio of 1D structure enable CNTs to form a stable interconnected network even at stretching state, making them popular for constructing stretchable energy storage devices.

Similar to graphene, CNTs are commonly produced by the chemical vapor deposition method. During growth, a substrate with catalyst particles is placed in a heated furnace with a supply of carbon feedstock gas and hydrogen gas, and CNTs are directly grown on the substrate, showing a random or aligned orientation. Numerous metals, including Fe, Co, and Ni, can

be used as catalysts for growing CNTs, and their sizes and catalytic activities have a huge influence on the diameter and length of the CNTs, thus deciding the mechanical and electrical properties of produced CNTs.^[52] For example, by controlling the thickness of the catalyst layer and the growth time, people had fabricated CNTs with lengths ranging from 300 to 900 μm , leading to the resistances varying from 300 to 1200 $\Omega \text{ sq}^{-1}$ accordingly.^[53] Besides the chemical vapor deposition method, CNTs also can be produced by arc discharge and laser ablations, but these methods commonly perform low yield and low purity, which prevent their large-scale applications.^[54,55]

To make full use of the produced CNTs, they are commonly dispersed in a solution to form a suspension followed by vacuum filtration, spray coating to produce thin conductive films.^[56,57] Thanks to the large length to diameter ratio, the produced CNT film can achieve a uniform electrical conductivity. To further increase the electrical conductivity of the CNT film, aligned CNT sheet produced by dry drawing from the CNT array has attracted increasing interest in recent years.^[58] Compared with the CNT film made of randomly dispersed CNTs, the CNT film made by dry drawing showed a highly aligned structure, i.e., almost all CNTs showed the same orientation, and they are connected end by end, providing a fast electron transfer channel along the CNT-aligned direction. However, the resistance perpendicular to the CNT-aligned direction is relatively high. Cross-stacking several layers of CNT sheets can overcome this shortcoming and the produced CNT film performs higher electrical conductivity and mechanical strength.^[59] Moreover, they can be used as flexible and conductive scaffolds to wrap active materials directly, paving the way for high electrochemical performances in energy storage devices.

CNT fiber is another essential 1D material for constructing fiber energy storage devices due to its high flexibility and conductivity. Floating chemical vapor deposition and dry spinning from CNT array are the two most adopted methods to produce CNT fibers.^[60,61] For the former method, CNT fiber is spun from a vertical chamber, in which CNT aerogel is first produced by chemical vapor deposition. As for the dry-spinning method, a CNT sheet is drawn out from the CNT array and then twisted into a fiber. Compared to the first method, the CNT fiber's mechanical and electrical properties can be easily modified by various post-treatment methods.^[62–64] Moreover, active materials can be easily loaded on the CNT sheet before twisting to produce hybrid fiber electrodes, simplifying the fabrication process of fiber energy storage devices, especially for batteries.^[65]

2.3. Other Carbon Materials

Beyond graphene and CNT, other carbon materials, such as carbon black, mesoporous carbon, carbon paper, and carbon fiber, are also widely used in energy storage devices.^[39,66–68] Carbon black is commonly used as conductive additives to improve the conductivity of the electrode.^[66] For example, through the addition of carbon black as conductive filler, a CNT/carbon black/polymer composite showed much lower sheet resistance than CNT/polymer composite, mainly because carbon black reduced the tunneling distance and decreased contact resistance among CNT junctions in the polymer

matrix.^[69] While, mesoporous carbon is broadly used as electrode material to construct supercapacitors because of its large specific area and sustainable conductivity.^[70] Meanwhile, other elements or active materials can be easily doped or incorporated with mesoporous carbon due to the open structure, resulting in supercapacitors with higher capacitance.^[67,71–73] As for the carbon paper, carbon fiber, and carbon cloth, they are commonly used as current collectors to assemble energy storage devices.^[74–77] Take carbon cloth for an example, attributed to their 3D structures and stable chemical features, active materials including conductive polymers and metal oxides can be directly deposited on carbon cloth to improve their energy storage performances.^[78] For instance, after in situ growth of MnO₂ on carbon cloth electrodes, the specific capacitance of the resulting supercapacitor reached 463 F g⁻¹, 99.7% of which can be maintained after cycling for 5000 cycles.^[79]

3. General Strategies to Prepare Stretchable Carbon-Material-Based Electrodes

Although carbon materials display both high conductivity and electrochemical performance, they are generally intrinsically inelastic. To this end, two general strategies have been developed to prepare stretchable carbon-material-based electrodes (Figure 2): i) composite with elastomers and ii) design of stretchable structures.

3.1. Composite with Elastomer

There are two main approaches to composite carbon materials with elastomers to obtain stretchable electrodes, i.e., mixed

with elastomer in bulk (Figure 2a-i) and embedded in/attached on the surface of elastomer (Figure 2a-ii).

The bulk-mixing method usually starts with the preparation of a uniformly blended solution of carbon material and elastomer. Below the saturation point, increasing the content ratio of carbon-based fillers can significantly improve the electrical conductivities of composite electrodes. Beyond the saturation point, the further increase of carbon material filler may aggregate together to decrease their mechanical strengths.^[80,81] For example, an elastic composite film with 20 wt% CNTs and carbon black particles as fillers showed a rupture point of about 400%, while a slight increase to 22 wt% of the carbon material fillers made it impossible to form a stretchable composite film.^[69] Although the bulk-mixing method is simple, the resulting composite electrodes generally show lower electrical conductivity and electrochemical activity, as only a few active points are exposed.

Compared with the bulk-mixing method, the embedded/attached method can obtain stretchable composite electrodes simultaneously with high electrical conductivity, electrochemical activity, and tensile stability. For the embedded method, carbon materials are usually dispersed in an aqueous solution or alcoholic solution to obtain a mixed suspension. The mixed suspension is then coated on a smooth substrate by different fabrication processes such as spin coating, spray coating, and drop casting.^[82,83] After drying and forming a conductive film, the elastomer precursor solution is subsequently coated on the conductive film. The composite electrode is finally obtained by peeling off the cured elastomer from the smooth substrate. Some carbon material films, e.g., CNT sheet, have good adhesion to elastic polymer substrates and can be attached directly to their surfaces.^[84,85] For carbon materials embedded in/attached on the surface, the resulting composite electrodes usually show

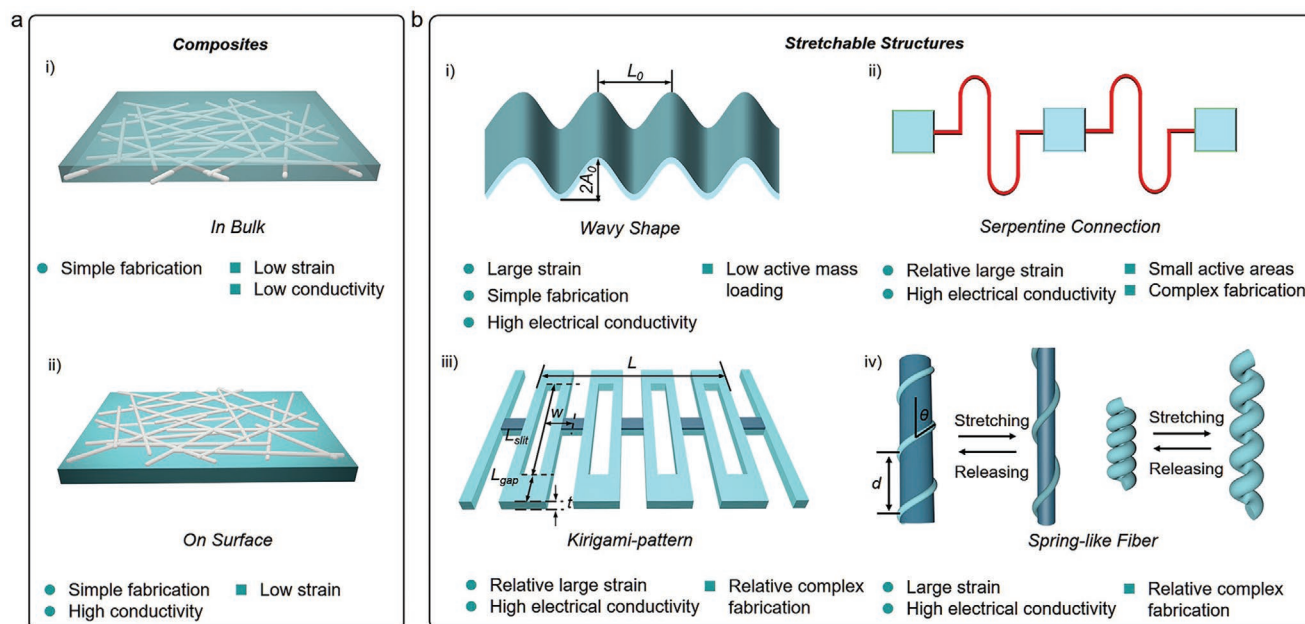


Figure 2. Schematic illustration of the general strategies to prepare stretchable carbon-material-based electrodes and their corresponding advantages and disadvantages. a) Composite carbon materials with stretchable elastomers, i) in bulk and ii) embedded/attached on surface. b) Stretchable structures formed by designing i) wavy, ii) serpentine, iii) kirigami-patterned, and iv) spring-like structures.

high electrical conductivities that are critical for the realization of high-performance energy storage devices.

3.2. Design of Stretchable Structures

The structure design is another effective method to fabricate stretchable devices. Wavy, serpentine, kirigami-patterned, and spring-like structures have been the most investigated because of their relatively easy operation and universalities.

3.2.1. Wavy Structure

Generally, wavy electrodes (Figure 2b-i) are produced by coating freestanding carbon material film, e.g., graphene and CNT films, on prestretched elastomers, followed by releasing to their initial states.^[33,86,87] Tensile strains are achieved mainly through the change in the amplitude and wavelength of the wavy structure and several analytic models have system discussed the relationship between wavelength and amplitude.^[88–91] A representative analytic model in the framework of finite deformation theory shows

$$\lambda_{\text{app}} = \frac{2\pi h_f (1 + \varepsilon_{\text{app}})}{(1 + \varepsilon_{\text{pre}})(1 + \varepsilon_{\text{app}} + \xi)^{1/3}} \left(\frac{\bar{E}_f}{3\bar{E}_s} \right)^{1/3} \quad (1)$$

$$A_{\text{app}} = \frac{h_f \sqrt{(\varepsilon_{\text{pre}} - \varepsilon_{\text{app}}) / \varepsilon_c - 1}}{(\sqrt{1 + \varepsilon_{\text{pre}}})(1 + \varepsilon_{\text{app}} + \xi)^{1/3}} \quad (2)$$

$$\varepsilon_c = \frac{1}{4} \left(\frac{3\bar{E}_s}{\bar{E}_f} \right)^{2/3} \quad (3)$$

$$\bar{E} = \frac{E}{1 - \nu^2} \quad (4)$$

And

$$\xi = \frac{5(\varepsilon_{\text{pre}} - \varepsilon_{\text{app}})\varepsilon_{\text{pre}}(1 + \varepsilon_{\text{pre}})}{32} \quad (5)$$

where the subscripts f and s represent the thin conductive carbon film and the elastic substrate, respectively; h_f is the thickness of the thin film, ε_c is the critical strain for the buckling to occur and is extremely small, \bar{E} is the plane-strain modulus with E and ν denoting Young's modulus and Poisson ratio, respectively.^[88] When a tensile strain is applied to the buckled thin-film system, a fracture will occur when $\varepsilon_{\text{app}} = \varepsilon_{\text{pre}} + \varepsilon_{\text{fracture}}$ is reached, where $\varepsilon_{\text{fracture}}$ is the fracture strain of thin film. As a result, the stretchability of the final device is $\varepsilon_{\text{stretchability}} = \varepsilon_{\text{pre}} + \varepsilon_{\text{fracture}}$. Thereby, the stretchability of these composite electrodes increases with increasing prestrain.^[91,92] It is also possible to produce biaxially stretchable electrodes by prestretching the substrate biaxially.^[93–95] For instance, a crumpled vertically aligned CNT array was transferred onto a biaxially prestretched elastomer to produce a wavy composite electrode that could be stretched biaxially by $300\% \times 300\%$ for thousands of cycles.^[95]

Besides the prestretching process, the template method has also been used to synthesize wavy electrodes. Thin conductive graphene sheets can be coated or directly grown on wavy templates to produce stretchable composite electrodes.^[96,97] For example, when transparent wavy graphene was prepared on wrinkle Cu substrate, a stretchable graphene electrode that can be stretched by up to 40% could be produced.^[98] The electrical conductivity of the resulting graphene electrode was higher than that produced by the prestretching method under the same strain. However, compared with the prestretching method, the template method generally showed lower strains due to smaller amplitudes.^[33,98,99]

3.2.2. Serpentine Structure

Stretchable devices with serpentine structure generally consist of carbon-material-based electrodes and photolithography-produced interconnected metallic serpentine wires, both of which are mounted or embedded in elastomers. Compared with the wavy structure, the serpentine structure offers stretchable property mainly through the in-plane deformation of conductive serpentine wires rather than the relatively rigid functional components. Therefore, the resulting stretchable electrodes shared higher stability.^[100,101] Figure 2b-ii shows a typical schematic design of a stretchable serpentine structure with several repeat units. The geometry of the unit cell can be described by four independent parameters, i.e., arc radius, width, arm length, and arc opening angle. Different combinations of the four parameters can induce the units with different geometries, demonstrating the diversity of the serpentine designs to meet different requirements.^[88] The mechanical behaviors of the serpentine structure with different unit geometries are quite different, but the stretchability of the final electrode ($\varepsilon_{\text{electrode}}$) can be evaluated by the following equation

$$\varepsilon_{\text{electrode}} = \left(1 - \sqrt{\frac{S_a}{S_t}} \right) \varepsilon_{\text{interconnect}} \quad (6)$$

where $\varepsilon_{\text{interconnect}}$ is the stretchability of the interconnected part; S_a and S_t are the area of the functional part and the total area of the electrode, respectively.^[102,103] It can be seen from Equation (6) that the stretchability of the whole electrode is inversely proportional to the area of the functional part. Therefore, the serpentine interconnects should be carefully designed to balance electronic function and stretchability. Furthermore, based on fractal designs, the researchers may introduce the serpentine configuration as the first-order structure and made the second, third, and even fourth structures according to the self-similar geometry.^[88] During stretching, these units will unravel orderly, enabling the device a larger stretchability.

3.2.3. Kirigami-Patterned Structure

The kirigami-patterned structure, inspired by the art of paper cutting, combines folding, cutting, and other manufacturing technologies to define stretchable patterns.^[104] A commonly used stretchable kirigami pattern, which consists of many cuts

with periodic parallel distributions, is shown in Figure 2b-iii. Upon stretching, the long “bridges” of the kirigami pattern are deformed longitudinally to accommodate large strains, similar to the serpentine structure. However, as there is no need to bond the kirigami pattern on any substrate, the deformations of the kirigami pattern are not limited in-plane.

The stretchability of the kirigami-patterned structure can be discussed with the beam model, and the film displacement associated with beam bending d_{total} , is proportional to the total load, P , of the film, which can be described as

$$d_{\text{total}} = \frac{N_c P (L_{\text{slit}} - L_{\text{gap}})^3}{N_r 8Ewt^3} \quad (7)$$

where N_c and N_r are the row and the column numbers of the cell units, respectively; E , w , t are Young's modulus, beam width, and film thickness, respectively.^[105] L_{slit} and L_{gap} are slit length and the gap between the slits (noticing the out-of-plane bending of each beam with a rotation is not considered in this formula). According to the formula, the bending property of each beam contributes to the final stretchability of the electrode and it is mainly dependent on the material (E) and geometry (e.g., w and t). Also, the final mechanical property is proportional to the column-/row-number ratio (N_c/N_r). When the rotation of each beam is considered (i.e., deformation is not limited in the plane), the final displacement can be given by the Pythagorean theorem

$$d_{\text{actual}} = \sqrt{L^2 + d_{\text{total}}^2} - L \quad (8)$$

where L is the film length before stretching. The above formula is more accurate when the deformation is very high to lead the beam units to rotate. Unpredictably, the strain-induced deformation can be uniformly dissipated in most regions of the whole pattern even at a large strain, according to the finite element analysis. Therefore, although the connecting points may show large strain concentrations, the whole device can maintain high conductivity and stability under stretching.^[106] To this end, a variety of carbon-material-based energy storage devices had been made stretchable by designing the kirigami-patterned structure.^[105,107,108] For example, a stretchable supercapacitor that can be stretched to 400% with kirigami-patterned CNT/MnO₂ electrode had been achieved by using this common strategy, and the capacitance can be well maintained even after stretching for 10 000 cycles.^[109]

3.2.4. Spring-Like Structure

Fiber devices have attracted broad interests in wearable electronics. Compared with conventional planar devices, fiber devices demonstrate unique properties. They can be easily integrated into complex systems by the well-studied weaving technology for large-scale applications, and woven into breathable textiles that may be closely attached to irregular or curved substrates such as skins.^[8] Different from the planar devices, fiber electrodes are shaped into helically coiled spring structures to achieve stretchability. The spring-like structure is typically

produced by wrapping CNT sheets or CNT fibers on elastic fiber substrates (Figure 2b-iv, left). The stretching range of the composite electrode increases with the decreasing angle θ , and the maximal strain (ϵ_{max}) can be briefly evaluated by the following equation

$$\epsilon_{\text{max}} = \sqrt{\frac{\pi^2 r^2}{d^2} + 1} - 1 \quad (9)$$

where r and d represent the radius of the fiber substrate and the pitch of the twisted conductive fiber, respectively.^[65] In other words, the maximal strain can be controlled by varying the values of r and d .

Although twisting conductive sheets or fibers on elastic fiber substrates can produce stretchable electrodes, the use of nonconductive elastomers increases the volume and weight of the entire device, leading to a low energy density. To overcome this challenge, an overtwisted structure (Figure 2b-iv, right) was proposed to realize stretchable fiber electrodes without using elastic substrates. For instance, a CNT fiber was directly overtwisted as the electrode of supercapacitor.^[110] The produced overtwisted coiled loops are extendable under stress and can automatically return to their original state. The obtained supercapacitor performed a stretch capacity of 100%. Although this approach improved the power density and energy density of the energy storage device, the stretching range was decreased due to the limited extending range of the coiled loops.

In summary, constructing carbon-material-based stretchable electrodes by compositing with elastomers has the advantages of simple fabrications and relatively stable electrochemical performances at low strains. However, they cannot meet the demand for large-strain applications. Adopting stretchable structure designs can significantly improve the stretchability of the electrodes, but they also have the drawback of complex fabrication. The strategies to produce a stretchable electrode should be carefully considered according to their specific applications.

4. Stretchable Supercapacitors Based on Carbon Materials

Supercapacitors are of great interest in wearable energy storage systems due to their combined advantages of high power density, long cycle life, and outstanding reversibility. According to the energy storage mechanisms, supercapacitors can be classified into electrochemical double-layer capacitors and pseudocapacitors.^[11,13,111] For the former, energy is stored/released by electrostatic charge accumulation/separate at the interfaces between electrode and electrolyte, and the surface area of the electrode plays a vital role in the performance. For the latter, energy is stored/released through a chemical process with reversible redox reactions, leading to a Faradic process between electrode materials and electrolytes.

A typical stretchable supercapacitor is fabricated by sandwiching gel electrolyte between two stretchable electrodes. Due to the large specific surface area and good conductivity, carbon materials, especially graphene and CNT can be directly used as electrodes to construct stretchable supercapacitors.^[95,112,113]

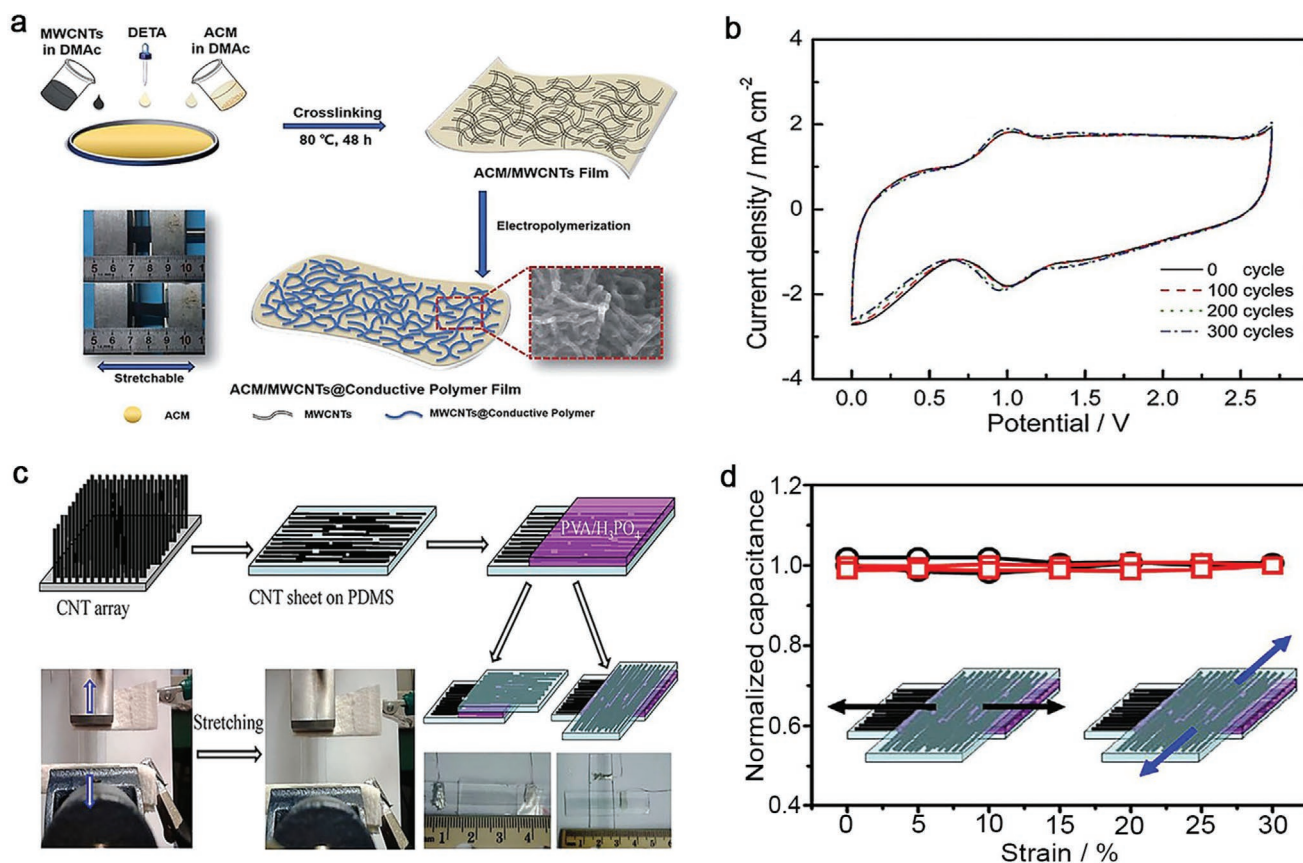


Figure 3. Stretchable supercapacitor based on carbon material/elastomer composite electrode. a) Schematics of the fabrication of stretchable ACM/MWCNTs@conductive polymer composite electrodes. b) Cyclic voltammogram curves of the stretchable supercapacitor based on ACM/MWCNTs@conductive polymer composite electrodes under various stretching cycles at 50% strain. (a) and (b) Reproduced with permission.^[114] Copyright 2018, The Royal Society of Chemistry. c) Schematics of the fabrication process for the stretchable supercapacitor based on CNT/PDMS composite electrodes. d) Normalized specific capacitance of the supercapacitor with cross-assembly as a function of tensile strain. (c) and (d) Reproduced with permission.^[84] Copyright 2014, Nature Publishing Group.

For example, a stretchable supercapacitor was developed based on intrinsically stretchable acrylate rubber (ACM)/MWCNT electrodes (Figure 3a).^[114] The ACM/MWCNT electrode was prepared by a chemical cross-linking method, which showed a good conductivity (9.6 S cm^{-1}) and stretchability (155%) with optimized MWCNT content of 35 wt%. The as-fabricated stretchable supercapacitor showed an energy density of 2.14 mWh cm^{-3} and good tensile stability of 500 stretching cycles at 50% strain (Figure 3b). Another example of a stretchable supercapacitor was developed by sandwiching a poly(vinyl alcohol) (PVA)/H₃PO₄ gel electrolyte between two CNT/poly(dimethylsiloxane) (PDMS) composite electrodes prepared by directly transferring CNT sheets onto elastic PDMS substrate (Figure 3c).^[84] The produced supercapacitor can be stretched by 30% for 100 cycles without capacity decreasing (Figure 3d).

Although the carbon materials can be directly used as electrodes to construct stretchable supercapacitors, the strain ranges of the supercapacitors are usually low and their specific capacitances degrade at high strains, so they are not suitable for the application fields where high strains occur. The design of stretchable structures may represent a promising method for highly stretchable supercapacitors. For example, a stretchable supercapacitor with a wavy structure was produced by the

prestretching strategy using two CNT films as electrodes and Laponite (synthetic hectorite-type clay)/graphene oxide cross-linked copolymer hydrogel as electrolyte (Figure 4a-i).^[115] The formed wavy-shaped CNT electrodes can achieve great tensile deformation up to 1000% without breaking the conductive network (Figure 4a-ii). As a result, the stretchable supercapacitor exhibited an intrinsically high strain of 1000% with well retained electrochemical performance (Figure 4a-iii). A stretchable supercapacitor was also produced with a serpentine structure as the serpentine conductive wires to realize the desired stretchability (Figure 4b-i).^[100] To obtain both higher energy density and stretchability, the SWCNT-based (Figure 4b-ii) energy-storing units were designed with a massive total area, but each unit is made as small as possible to decrease the stress concentration. Besides, the elastic serpentine conductive wire should also be optimized with a smaller area. As a result, the stretchable supercapacitor showed a stable electrochemical performance under stretching up to 30% without apparent decline (Figure 4b-iii,iv). The stretchable supercapacitor with a kirigami-patterned structure showed a similar island-bridge configuration to the supercapacitor with serpentine wires. Differently, active materials can also be loaded on the bridge to increase the output energy. For instance, a supercapacitor with

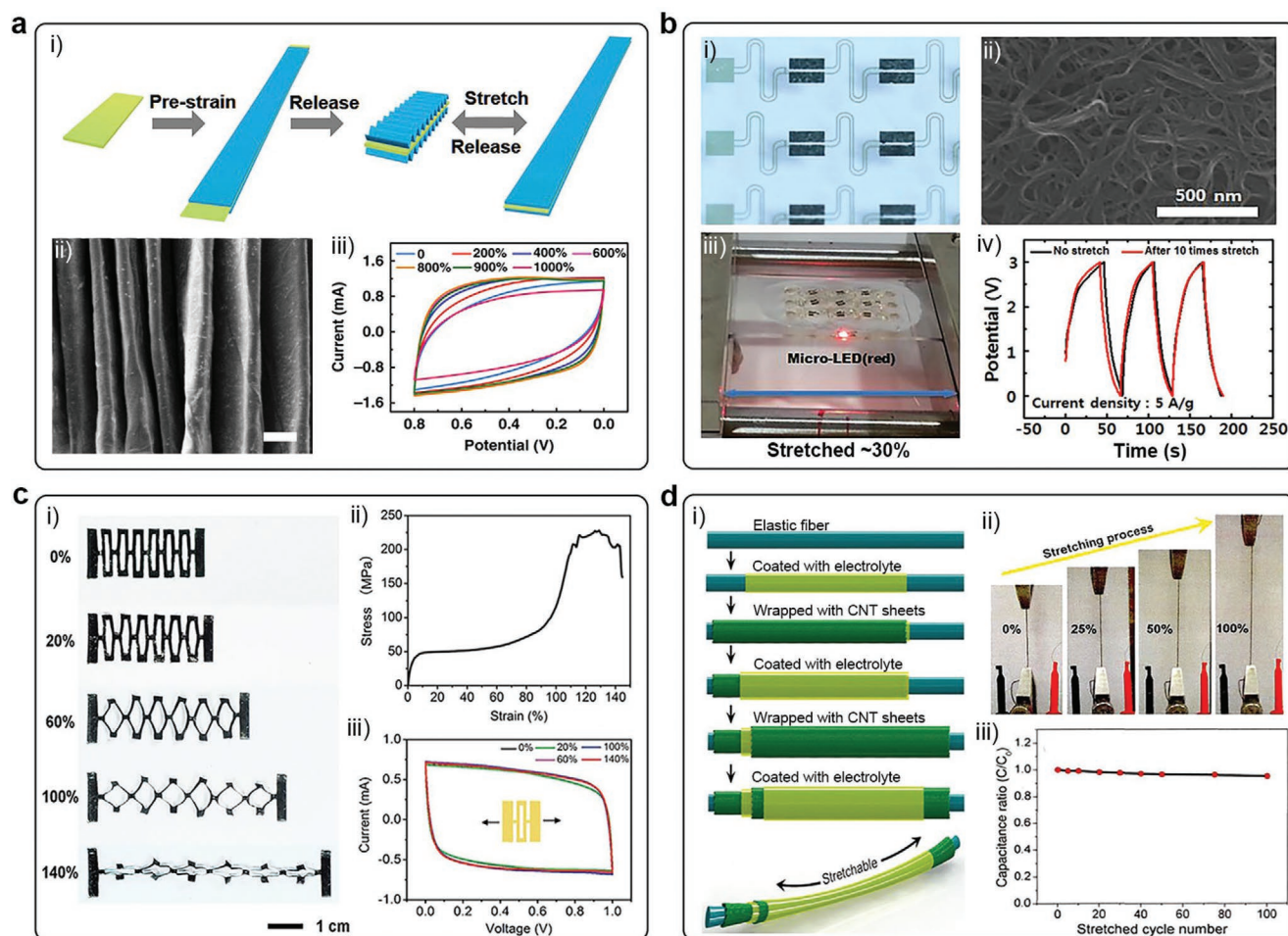


Figure 4. Stretchable supercapacitor from geometrically structured carbon-material-based electrode. a) Stretchable supercapacitor based on wavy structure. i) Schematic for the fabrication of a stretchable supercapacitor based on wavy CNT film electrode (scale bar: 200 μm) and iii) cyclic voltammograms of the supercapacitor being stretched from 0% to 1000%. Reproduced with permission.^[115] Copyright 2019, Nature Publishing Group. b) Stretchable supercapacitor based on serpentine structure. i) Photograph of a stretchable supercapacitor array with a serpentine structure as the serpentine conductive wires on a PDMS substrate. ii) SEM image of the SWCNT electrode. iii) Photograph showing the discharging state of the stretchable supercapacitor powering μ -LEDs under 30% stretched state. iv) Variation of galvanostatic charge/discharge curves at 5 A g^{-1} upon 10 times repetition of 30% stretching. Reproduced with permission.^[100] Copyright 2013, American Chemical Society. c) Stretchable supercapacitor based on kirigami-patterned structure. i) Photographs of the kirigami-patterned CNT electrode under increasing strains from 0% to 140%. ii) Stress-strain curve of the kirigami-patterned CNT electrode. iii) Cyclic voltammograms of the stretchable supercapacitor with increasing strains from 0% to 140%. Reproduced with permission.^[116] Copyright 2016, The Royal Society of Chemistry. d) Stretchable fiber supercapacitor based on spring-like structure. i) Schematics of the fabrication of a stretchable fiber supercapacitor based on CNT sheet electrodes. ii) Photograph of the supercapacitor with increasing strains from 0% to 100%. iii) Dependence of specific capacitance on cycle number at strain of 75%. Reproduced with permission.^[118] Copyright 2013, Wiley-VCH.

kirigami-patterned electrodes (Figure 4c-i,ii) could be stretched without fatigues in electrochemical properties.^[116] The cyclic voltammograms almost overlapped with increasing tensile strains from 0% to 140% (Figure 4c-iii).

Due to the flexible and wearable properties, fiber supercapacitors have received wide attention in recent years.^[110,117–120] They could be directly woven into clothes, enabling them to have special wearable applications, e.g., textile electronics.^[120] The stretchable fiber supercapacitor appeared by the design of coaxially wrapping two CNT sheets around an elastic PDMS fiber sandwiched with a PVA/ H_3PO_4 gel electrolyte layer (Figure 4d-i,ii).^[118] The stretchable fiber supercapacitor exhibited a specific capacitance of $\approx 20 \text{ F g}^{-1}$, and the electrochemical performance can be maintained by 95% under

100 stretching cycles at a strain of 75% (Figure 4d-iii). A stretchable fiber supercapacitor was also realized by coaxially wrapping the CNT sheet/polyaniline (PANI) composite electrode around a prestretched PDMS fiber substrate. It had achieved a higher specific capacitance of about 79.4 F g^{-1} after stretching at a strain of 300% for 5000 cycles.^[119]

Table 1 has summarized the electrochemical performance and stretchability of some representative stretchable supercapacitors based on carbon materials. CNT and graphene are the most commonly used carbon materials for stretchable supercapacitors.^[84,100,113,115,121,122] Conductive polymers, including PANI, polypyrrole (PPy), and poly(3,4-ethylenedioxythiophene):poly(styrenesulfonate) (PEDOT:PSS), and metal oxides (MnO_2 and MoS_2) have been

Table 1. The electrochemical performance and stability of representative stretchable supercapacitors based on carbon materials.

Electrode material	Carbon material content	Specific capacitance	Maximal strain	Electrochemical stability after stretching	Ref.
PANI deposited on CNT/PDMS composite film	10 wt%	159 F g ⁻¹	50%	≈100% at 50% strain, 95.6% after stretching for 500 cycles at 50% strain	[124]
Laser-induced graphene/PDMS composite films	–	650 μF cm ⁻²	50%	Slight decline after stretching to 50% strain	[121]
N-doped CNT array embedded in polyurethane	15.3 mg cm ⁻²	31.1 mF cm ⁻²	400%	98.9% at 400% strain, 96% after stretching for 1000 cycles at 200% strain	[122]
Graphene membrane attached on PDMS	30 μg cm ⁻²	3.3 mF cm ⁻² /55 F g ⁻¹	38%	≈100% at 38% strain, ≈90% after stretching for 1000 cycles at 20% strain	[113]
CNT/MoS ₂ composite film attached on PDMS	93.5 wt%	13.16 F cm ⁻³	240%	≈100% at 240% strain, 96% after stretching for 500 cycles at 100% strain, 91% after stretching for 500 cycles at 160% strain	[123]
Graphene/MoS ₂ composite film attached on PDMS	31.7 wt%	70 mF cm ⁻² /19.44 mF cm ⁻³	60%	87% after stretching for 300 cycles at 30% strain	[127]
CNT sheets attached on PDMS	1.2–1.4 μg cm ⁻²	7.3 F g ⁻¹	30%	≈100% after 100 stretching cycles at 30% strain	[84]
PPy/graphene foam attached on PDMS	1.6 ± 0.4 mg cm ⁻²	258 mF cm ⁻²	50%	69% at 50% strain, ≈88% after stretching for 100 cycles at 30% strain	[44]
Wavy CNT array/acrylic elastomer composite film	–	5 mF cm ⁻²	800%	≈100% at 800% strain, ≈100% after stretching for 1200 cycles at 300% strain	[95]
Wavy CNT film	–	9 mF cm ⁻²	1000%	≈110% at 900% strain; 87% at 1000% strain; 98% after stretching for 2000 cycles at 300% strain	[115]
Wavy graphene/PANI film	–	261 F g ⁻¹	30%	95% after stretching for 100 cycles at 20% strain	[97]
Kirigami-patterned CNT/MnO ₂ nanowire film	1.6 mg cm ⁻²	227.2 mF cm ⁻²	400%	≈98% after stretching for 10 000 cycles at 400% strain	[109]
Kirigami-patterned CNT/PANI film	95 wt%	42.4 F g ⁻¹	140%	≈100% after stretching for 45 000 cycles at 140% strain	[116]
Serpentine single-walled CNT film	1.48 μg cm ⁻²	55.3 F g ⁻¹	30%	≈100% at 30% strain, ≈100% after stretching for 10 cycles at 30% strain	[100]
CNT/PANI composite film wrapped on PDMS fiber	50 wt%	105.8 F g ⁻¹	400%	≈100% at 400% strain, 74.9% after stretching for 5000 cycles at 300% strain	[119]
Spring-like MnO ₂ /CNT/elastomer fiber	–	16.1 mF cm ⁻²	600%	90.3% at 600% strain, 97% after stretching for 100 cycles at 600% strain	[128]
Spring-like MnO ₂ /PEDOT:PSS/CNT and MoS ₂ /CNT fibers	–	278.6 mF cm ⁻²	100%	92% after stretching for 3000 cycles at 100% strain	[125]
Spring-like PPy/RGO/CNT fibers	–	25.9 mF cm ⁻³	100%	82.4% at 100% strain	[126]

further investigated to enhance the electrochemical performances of carbon-based supercapacitors.^[44,123–128] As a result, a variety of carbon-based stretchable supercapacitors have been developed rapidly in recent years, and their electrochemical and mechanical properties have also been greatly improved. However, the energy storage capacity of the supercapacitor is usually poor, so stretchable batteries become necessary and attract even more interest in recent years.

5. Stretchable Li-Ion Batteries Based on Carbon Materials

Compared with supercapacitors, Li-ion batteries exhibit higher energy densities and lower self-discharge losses, making them more favorable for power supply in wearable electronics.^[129,130]

Similar to stretchable supercapacitors, stretchable Li-ion batteries are usually made of two stretchable electrodes and gel electrolyte as the separator. The difference is that carbon-material-based conductors are mainly used as current collectors, which should further load active materials to construct stretchable electrodes.^[131]

For example, a stretchable current collector was first produced by embedding CNTs and carbon black particles into a poly(styrene)-*block*-poly(ethylene-*ran*-butylene)-*block*-poly(styrene) (SEBS) elastomer with highly conductive Ag microflakes as the top layer (Figure 5a,b).^[132] Two stretchable electrodes were then fabricated by spray coating LiMn₂O₄ (LMO)/carbon black and ε-Li_xV₂O₅/carbon black on the stretchable current collector, respectively. The full stretchable Li-ion battery was finally fabricated by compositing the two stretchable electrodes and polyacrylamide hydrogel electrolyte

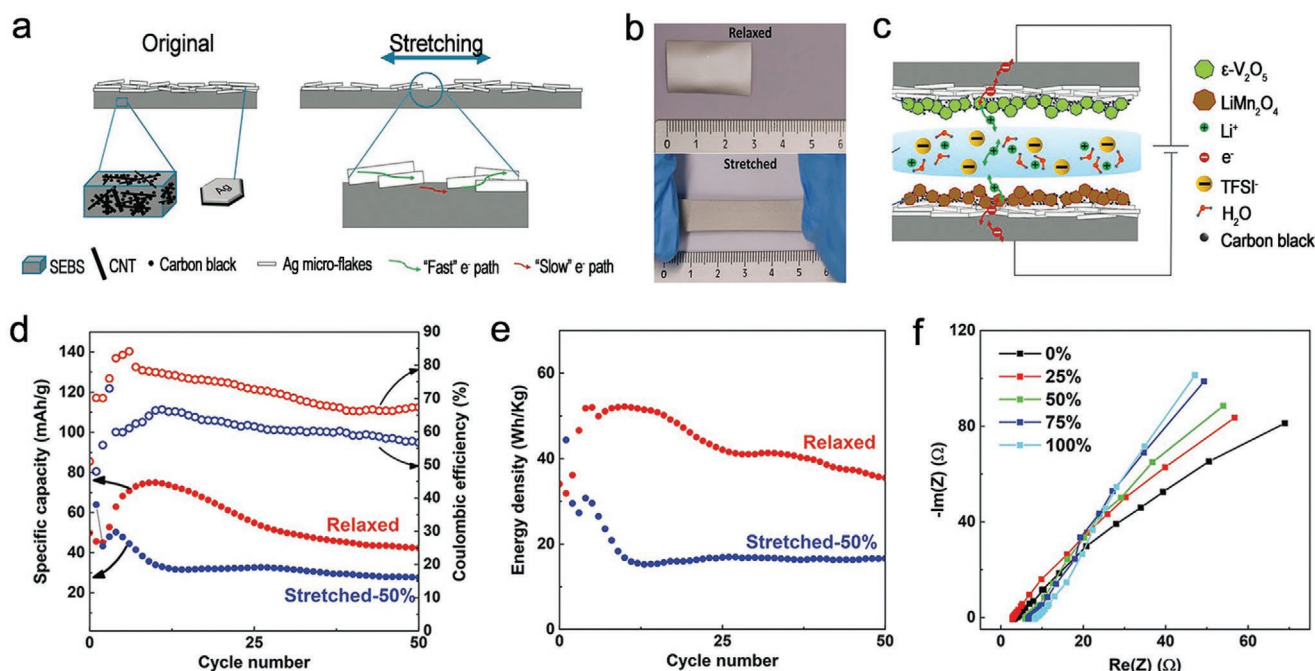


Figure 5. Stretchable Li-ion battery based on carbon material/elastomer composite electrode. a) Schematic illustration of a stretchable current collector using SEBS matrix and carbon black/CNT/Ag microflake conductive fillers for Li-ion battery. b) Photograph of the current collector before and after stretching. c) Schematic illustration of a stretchable Li-ion battery based on LiMn₂O₄/carbon black/stretchable current collector and ε-Li_xV₂O₅/carbon black/stretchable current collector composite electrodes. d,e) Specific capacity and energy density of the stretchable battery at relaxed and 50% stretched states over 50 galvanostatic cycling cycles, respectively. f) Nyquist plots of the stretchable Li-ion battery at different strains. Reproduced with permission.^[132] Copyright 2019, Wiley-VCH.

into a PDMS elastomer package (Figure 5c). The resulting stretchable Li-ion battery exhibited a specific capacity of 43 mAh g⁻¹ and an energy density of 35 Wh kg⁻¹, which were maintained by about 65% and 49% after stretching to 50%, respectively (Figure 5d,e). The main reason for the capacity and energy loss at the stretched state lies in the increased internal resistance of the battery, which can be concluded from the electrochemical impedance spectroscopy, where the slopes of Nyquist plots increased with the increasing degree of stretching (Figure 5f).

Although the above fabrication process is simple, the stretchability of Li-ion battery is typically lower than 100%, and the capacity degrades largely at high strains. This problem mainly comes from the increased resistance of the current collector and the detachment of active materials during the stretching process. To guarantee the stable electrochemical performances of Li-ion batteries during stretching, active materials should be efficiently and strongly bonded onto current collectors. Electrically conductive CNT sheets are ideal current collectors for Li-ion batteries as active materials can be closely bundled and stabilized by the flexible and conductive CNT scaffolds.^[87,94] For example, a stretchable Li-ion battery was fabricated by sandwiching gel electrolyte between two wavy CNT sheet/Li₄Ti₅O₁₂ (LTO)-CNT and CNT sheet/LMO-CNT composite electrodes (Figure 6a-i,ii).^[87] The charge/discharge voltage profiles of the battery after stretching for 200 cycles can remain stable after various numbers of cycles (Figure 6a-iii). The design of the serpentine and kirigami-patterned structure

is also effective in improving the tensile stability. As a representative example, Rogers and co-workers have developed a stretchable Li-ion battery with self-similar serpentine interconnects (Figure 6b-i), enabling reversible levels of stretchability up to 300%, while maintaining capacity densities of about 1.1 mAh cm⁻² (Figure 6b-ii,iii).^[101] To construct a stretchable Li-ion battery with kirigami-patterned structure, all of the components should be produced in the same pattern and perfectly laminated together. For instance, two microhoneycomb graphene-CNT/active material composite electrodes are laminated with a physically cross-linked gel electrolyte to produce the desired battery (Figure 6c-i), and it could be stretched by over 50% with stable specific capacities of ≈120 mAh g⁻¹ (Figure 6c-ii).^[133]

Similar to the fiber supercapacitor, a stretchable fiber Li-ion battery has also been developed by remolding the fiber electrode into spring-like shapes.^[65,110,134] For example, two aligned CNT composite fibers were first produced by incorporating LTO and LMO nanoparticles into aligned CNT fibers that serve as anode and cathode, respectively.^[65] A stretchable fiber Li-ion battery was then produced by winding these two CNT composite fibers on an elastomer substrate, followed by coating with a layer of gel electrolyte (Figure 6d-i,ii). The spring-like structure enabled the composite fiber electrode with high stretchability, and the change in electrical resistance was less than 10% after stretching for 100 cycles at a strain of 600%. As a result, the stretchable fiber Li-ion battery exhibited a record strain of 600% (Figure 6d-iii). Another example of fabricating

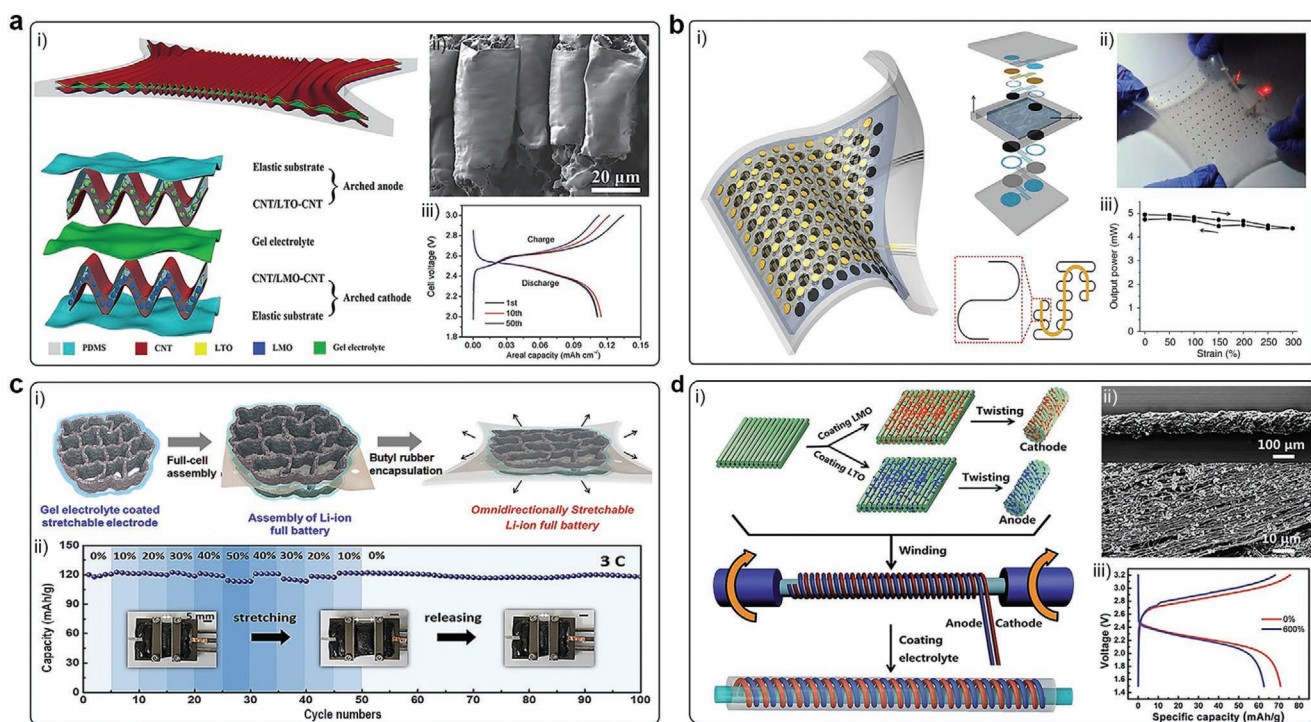


Figure 6. Stretchable Li-ion battery from geometrically structured carbon-material-based electrode. a) Stretchable Li-ion battery based on wavy structure. i) Schematics of a stretchable Li-ion battery based on wavy CNT sheet/LMO–CNT and CNT sheet/LTO–CNT composite electrodes. ii) SEM image of the wavy CNT sheet/LMO–CNT composite electrode. iii) Voltage profiles of the stretchable Li-ion battery after 200 stretching cycles at various numbers of charge–discharge cycles. Reproduced with permission.^[87] Copyright 2016, Wiley-VCH. b) Stretchable Li-ion battery based on kirigami-patterned structure. i) Schematics of a stretchable Li-ion battery and the exploded view layout of the various layers in the battery. ii) Photograph of the battery connected to a red LED while biaxially stretched to 300%. iii) Output power of the battery as a function of applied biaxial strain. Reproduced with permission.^[101] Copyright 2013, Nature Publishing Group. c) Stretchable Li-ion battery based on kirigami-patterned structure. i) Schematics of the fabrication of the stretchable Li-ion battery based on two microhoneycomb graphene–CNT/active material composite electrode. ii) Discharge capacity of the stretchable battery with applied strain ranging from 0% to 50% for 100 cycles. Reproduced with permission.^[133] Copyright 2020, American Chemical Society. d) Stretchable fiber Li-ion battery based on spring-like structure. i) Schematic illustration to the fabrication of a stretchable fiber Li-ion battery based on fiber CNT/LMO and CNT/LTO electrodes. ii) SEM images of fiber CNT/LMO electrode at low and high magnifications, respectively. iii) Charge/discharge profiles of the stretchable fiber Li-ion battery before and after stretching to 600% at a current density of 0.1 mA cm^{-2} . Reproduced with permission.^[65] Copyright 2014, The Royal Society of Chemistry.

a stretchable fiber Li-ion battery is to overtwist the CNT composite fiber electrode to produce coiled loops.^[110] Compared with the former strategy, the latter generally presents higher energy densities because no nonactive elastic substrates are required. For instance, for the same CNT/LMO and CNT/LTO composite fiber electrodes, the battery with an overtwisted configuration can achieve an improvement of 600% in the linear specific capacity.

Table 2 compares the stretchable Li-ion batteries developed in recent years. Although their capacities are much higher than those of stretchable supercapacitors, it should be noted that the capacities of stretchable Li-ion batteries lag far behind commercial Li-ion batteries. The main reason lies in those nonactive elastic components introduced in the electrodes, which significantly increase the mass and volume. Moreover, the stretchability of Li-ion batteries is generally lower than those of stretchable supercapacitors, which is attributed to the use of inherently rigid active materials that reduce elasticity. Therefore, more efforts are needed to improve the comprehensive performance of stretchable Li-ion batteries from the aspects of material synthesis and structure design.

6. Stretchable Metal–Air Batteries Based on Carbon Materials

Metal–air batteries including Li–air, Zn–air, and Al–air batteries have been identified as promising energy storage candidates due to their extremely high theoretical energy densities.^[135] Traditional metal–air batteries consist of a metal anode (e.g., Li, Zn, and Al), a porous air cathode, and an electrolyte. Carbon materials are one of the most used air cathodes for metal–air batteries due to their high specific surface area and excellent oxygen catalytic performance.^[136–140] Recently, some efforts have also been devoted to developing stretchable metal–air batteries by using stretchable carbon-material-based electrodes for powering wearable devices.

For example, a stretchable Li–air battery has been developed by designing a wavy air cathode made of aligned CNT sheets, a lithium array electrode, and a polymer gel electrolyte (Figure 7a,b).^[136] The as-fabricated stretchable Li–air battery exhibited a high discharge voltage plateau of 2.57 V, which remained almost unchanged over 180 discharging/charging cycles at a cutoff capacity of 500 mAh g^{-1} . Notably,

Table 2. The electrochemical performance and stability of representative stretchable Li-ion batteries based on carbon materials.

Electrode material	Carbon material content	Specific capacity	Maximal strain	Electrochemical stability after stretching	Ref.
Polyurethane/Au/CNT/polyimide and polyurethane/Au/CNT/LMO composite films	–	100 mAh g ⁻¹	30%	72% after cycling for 10 cycles at 30% strain	[131]
Polyimide and LMO coated on CNT/carbon black/Ecoflex composite films	10 wt% for CNT; 10 wt% for carbon black	89 mAh g ⁻¹	100%	80% at 100% strain, ≈100% after cycling for 90 cycles under various amounts of strain (0–100%)	[69]
PDMS sponge/carbon black/LTO and PDMS sponge/carbon black/LiFePO ₄ composites	10 wt%	100 mAh g ⁻¹ for LTO; ≈120 mAh g ⁻¹ for LiFePO ₄	80%	82% after stretching for 500 cycles at 80% strain for LTO; 91% after stretching for 500 cycles at 80% strain for LiFePO ₄	[130]
Wavy CNT/LTO/PDMS and CNT/Li(Ni _{1/3} Co _{1/3} Mn _{1/3})O ₂ /PDMS composite films	5 wt%	0.52 mAh cm ⁻²	150%	96% after stretching for 2000 cycles at 150% strain	[94]
Wavy CNT sheets/LTO–CNT/PDMS and CNT sheet/LMO–CNT/PDMS composite films	–	175 mAh g ⁻¹	400%	97% after stretching for 200 cycles at 400% strain	[87]
Serpentine acetylene black/LTO and acetylene black/LiCoO ₂ composite films	10 wt%	1.1 mAh cm ⁻²	300%	≈90% at 300% strain	[101]
Overtwisted spring-like CNT/LTO and CNT/LMO composite fibers	–	2.2 mAh m ⁻¹	100%	85% at 100% strain, ≈100% after stretching for 300 cycles at 50% strain	[110]
Spring-like CNT/LTO and CNT/LMO composite fibers wrapped on PDMS fiber	42.3 and 16.4 wt%	91.3 mAh g ⁻¹	600%	88% at 600% strain, 90% after stretching for 100 cycles at 200% strain	[65]

the electrochemical performance can be well maintained during and after stretching with strains up to 100% (Figure 7c). Another wavy structure was proposed to develop a stretchable Zn–air battery.^[141] Briefly, a Au macrofoil/CNT paper air cathode and a Zn/CNT paper anode were first prepared by attaching Au macrofoil and depositing zinc onto CNT paper substrate, respectively. The as-prepared electrodes were then attached to a prestretched hydrogel polyelectrolyte, followed by releasing the strain to form a Zn–air battery with a wavy structure. The resulting battery exhibited an intrinsically high strain of 300% and high compression of 85% with well retained electrochemical performance. The design of the serpentine structure has been also developed for stretchable metal–air batteries. For instance, a stretchable Zn–air battery was fabricated by assembling Zn foils and Co₃O₄/carbon cloth air electrode array with serpentine conductive wires in an Ecoflex thin film (Figure 7d).^[142] It can be stretched by 125% without noticeable structure damage (Figure 7e), and the average discharge voltages remained almost unchanged in the stretching/releasing process (Figure 7f). Similarly, the kirigami-patterned structure was also used to fabricate metal–air batteries.^[143] By employing an Al foil and a carbon black composite placed on a cellulose scaffold as substrate, a shape-reconfigurable Al–air battery was developed and can be stretched to 172%. A high output voltage of 10.3 V can be achieved with 16 unit battery cells connected in series (Figure 7g–j).^[144]

Stretchable fiber metal–air batteries were also developed at the same time.^[137,138] As shown in Figure 7k, a strategy was proposed to sequentially coat a gel electrolyte and a cross-stacked CNT/Ag sheet onto a spring-like Al anode to obtain the fiber Al–air battery.^[138] The battery was stretched to 30% without obvious damages in structure, and the output voltage was also maintained above 1 V (Figure 7l). The stretchable fiber structure enabled it to exhibit some unique wearable applications. For instance, two stretchable fiber Al–air batteries were woven into

a flexible textile to power a light-emitting-diode (LED) watch worn around a human wrist (Figure 7m). Besides the Al–air battery, a stretchable fiber Zn–air battery was also developed by the same strategy using a CNT sheet/RuO₂ air cathode and a spring-like Zn anode.^[137]

Table 3 compares the electrochemical and mechanical performances of representative metal–air batteries. The specific capacity is much improved, but the stretchability of metal–air batteries is a bit lower, which is mainly limited by the poor mechanical property of metal anode. Although a novel metal–air battery using liquid metal as an anode was proposed to improve the stretchability, it only can be stretched to 100%, which is still lower than stretchable supercapacitors and Li-ion batteries.^[145] Thus, developing an effective method to endow the metal anode with high stretchability is still in urgent need.

7. Other Stretchable Batteries Based on Carbon Materials

Stretchable Na-ion batteries, K-ion batteries, and Zn-ion batteries have received increasing attentions in recent years, due to their unique advantages such as abundant element reserves, cheap raw materials, and high safety.^[18,146,147] The structural design and device construction of these stretchable batteries are mostly inseparable from carbon materials. For instance, an all-stretchable-component Na-ion battery had been developed on the basis of two graphene-modified PDMS sponge electrodes and an elastic gel membrane.^[18] The graphene-modified PDMS sponge was fabricated by immersing stretchable PDMS sponge in graphene oxide solution, followed by exposing the dried PDMS/graphene oxide sponge to HI vapor to change the graphene oxide into reduced graphene oxide (RGO). Commercial hard carbon and preprepared 2D VOPO₄ nanosheets were used as anode and cathode materials, respectively. The Na-ion battery

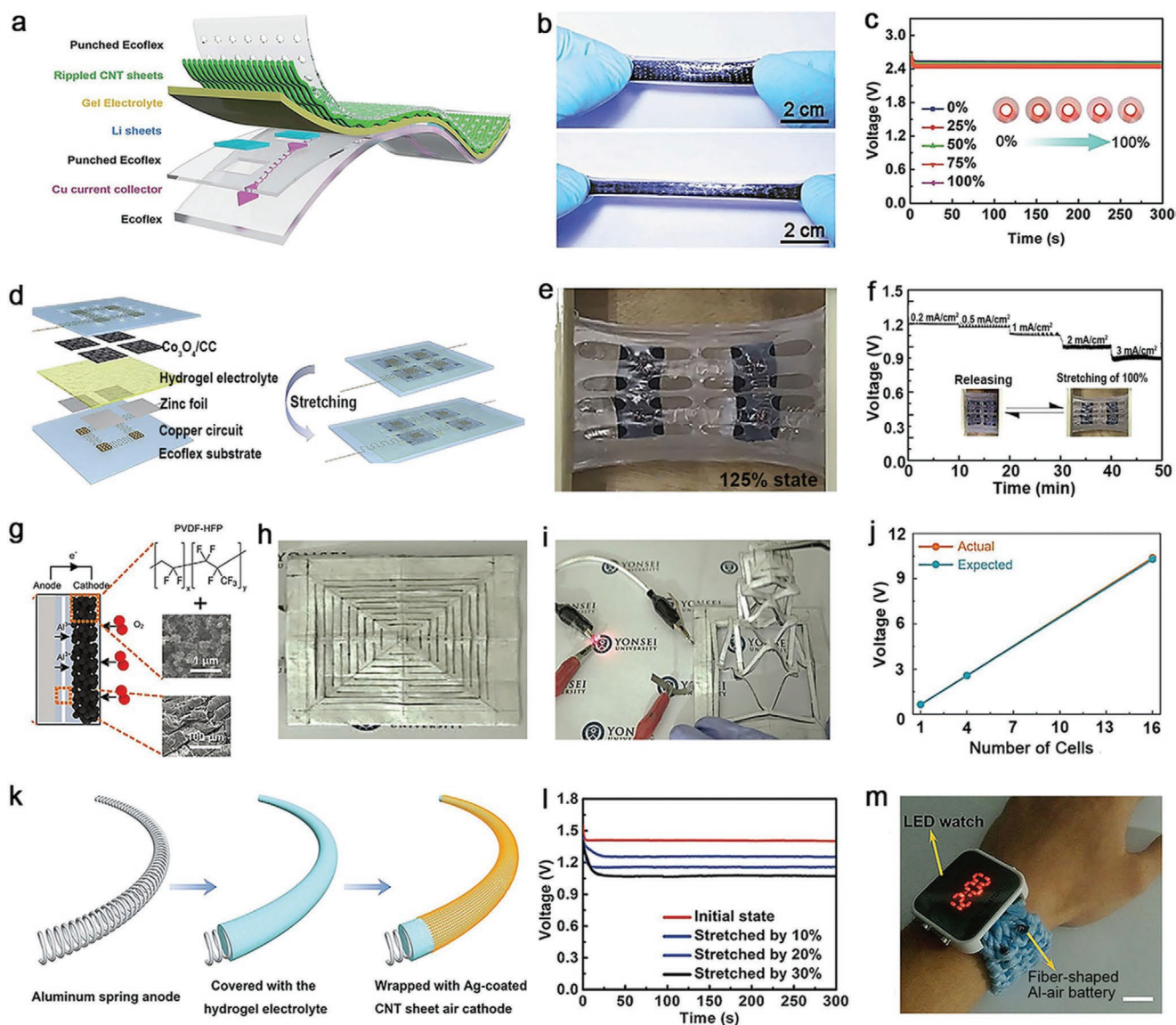


Figure 7. Stretchable metal–air battery from geometrically structured carbon-material-based electrode. a) Schematics of a stretchable Li–air battery based on rippled CNT sheet electrode. b) Photographs of the stretchable Li–air battery before and after stretching. c) Discharge curves of the stretchable Li–air battery under increasing strains from 0% to 100%. (a–c) Reproduced with permission.^[136] Copyright 2016, The Royal Society of Chemistry. d,e) Schematics and photograph of a stretchable Zn–air battery based on Zn foils and Co_3O_4 /carbon cloth air electrode array with serpentine conductive wires in an Ecoflex thin film. f) Rate discharge curves of the battery with increasing strains from 0% to 125% at different discharge current densities. (d–f) Reproduced with permission.^[142] Copyright 2017, Elsevier Ltd. g) Schematics of the structure of a shape-reconfigurable Al–air battery. h,i) Photographs of a shape-reconfigurable Al–air battery with kirigami-patterned structure to turn on a red LED before and after 3D stretching. j) Real and expected trends of the open-circuit voltage for series-connected shape-reconfigurable Al–air battery. (g–j) Reproduced with permission.^[144] Copyright 2017, Wiley-VCH. k) Schematic illustration to the fabrication of stretchable fiber Al–air battery based on CNT sheet electrode. l) Discharge curves of the Al–air battery under different stretching strains at a discharge current of 1 mA. m) Photograph of a commercial LED watch powered by two stretchable fiber Al–air batteries connected in series. (k–m) Reproduced with permission.^[138] Copyright 2016, Wiley-VCH.

exhibited a stable capacity of about 126 mAh g^{-1} at a current density of 50 mA g^{-1} . Graphene is mainly used as a conductive agent to construct the stretchable composite current collector. The as-fabricated battery can achieve tensile stability, e.g., the specific capacity can retain over 89% after 100 cycles of stretching to 50%. Another stretchable K-ion battery was developed from Na–K alloy and carbon powder composite anode.^[146] Here, the carbon powder can well connect with the Na–K alloy

to form an extremely stable liquid alloy–current collector interface and liquid alloy–liquid electrolyte interface. The main reason lies in hydroxides that were formed by the reaction of liquid alloy metal with trace water in the carbon particles enabling the composites strong viscosity and low surface tension, offering a facile approach to construct stretchable K-ion battery. The resulting K-ion battery can be stretched by over 200%. Stretchable Zn-ion batteries, predominantly aqueous Zn-ion

Table 3. The electrochemical performance and stability of representative stretchable metal–air batteries based on carbon materials.

Anode	Cathode	Carbon material content	Specific capacity	Maximal strain	Electrochemical stability after stretching	Ref.
Lithium array connected with spring-like Cu wire	Wavy CNT	≈14.1 μg cm ⁻²	7111 mAh g ⁻¹	100%	≈100% after stretching for 1000 cycles at 75% strain	[136]
Wavy shape zinc-deposited CNT paper	Wavy Au/CNT paper	The thickness of 20 μm	–	300%	≈100% at 300% strain	[141]
Zinc spring	CNT sheet loaded with RuO ₂	–	6 Ah L ⁻¹	10%	The discharge voltage was well maintained at 10% strain	[137]
Aluminum spring	CNT sheet loaded with Ag	≈48 wt%	935 mAh g ⁻¹	30%	≈70% of the initial discharge voltage at 30% strain	[138]
Liquid metal (90 wt% Ga + 10 wt% In)	Carbon fiber	98.2 wt%	214.8 mAh g ⁻¹	100%	≈100% of the initial discharge voltage at 100% strain	[145]

batteries, have also been reported in recent years due to their high safety for wearable applications. For example, a stretchable aqueous Zn-ion battery was developed by assembling Zn nanoflakes/Au@CNT paper electrode and NiCo hydroxide/Au@CNT paper electrode with hydrogel electrolyte.^[148] The as-fabricated battery can be stretched by up to 400%, and 87% of capacity can be maintained after stretching for 500 cycles.

8. Conclusions and Outlook

To summarize, focusing on carbon-material-based electrodes, we have highlighted the progress of stretchable energy storage devices which has been widely explored in recent years. Undeniably, CNT and graphene are the most used electrode materials for existing stretchable energy storage devices due to their large specific surface areas and high electrical and electrochemical properties. Moreover, two general strategies, i.e., compositing carbon materials with elastomers and designing stretchable structures, were compared in preparing stretchable electrodes. A range of stretchable energy storage devices including supercapacitors, Li-ion batteries, and metal–air batteries have been achieved. Although remarkable advances have been made in the development of stretchable energy storage devices with high strain performances, enormous challenges are hindering the realization of practical applications (Figure 8a).

From the perspective of the component for energy storage devices, the cost of the commonly used CNT and graphene in electrodes should be concerned. The cost of carbon nanotubes was quite high 20 years ago (45 \$ g⁻¹). However, with the increase of the market's demands and the development of large-scale production technology, the price has been largely decreased (0.1–25 \$ g⁻¹).^[47,149] As for graphene and its derivatives, they have achieved mass production of 2799 tons in 2017, and the cost is also largely reduced.^[150] Thus, we can conclude that the cost will be further reduced with the joint efforts of industry. Besides, stretchable polymer materials including PDMS, polyurethane, and Ecoflex are widely used as encapsulation layers for stretchable energy storage devices. However, the devices, especially Li-ion batteries, generally fail quickly because of their high water and oxygen transmission rates. Therefore, new encapsulation materials are urged

to achieve high stretchability and low water/gas permeability (Figure 8b).

Viewing from the entire device level, the electrochemical performances of the current stretchable energy storage devices are much lower than those of commercial counterparts (Figure 8c). One issue stretchable energy storage devices are facing is the delamination of active materials from the substrate during repeat stretching, leading to rapid energy density degradation. Therefore, developing novel methods or novel structures that can tightly bond active materials on the electrode still needs to be considered. Except for the stability, the energy densities of stretchable energy devices are lower than their counterparts. One of the most important and common reasons is that the used elastic substrate is several orders heavier than the electrode materials, leading to a much lower energy density. Developing a stretchable energy storage device with lightweight or even free of the elastic substrate will help solve this problem to a certain degree. Specifically, for supercapacitors, increasing the specific surface area of carbon materials or compositing with pseudocapacitance materials is useful to further improve their capacitance. For Li-ion batteries, the discovery of novel electrode materials with both high electrochemical and mechanical properties and the development of innovatory strategies to load more active materials in stretchable electrodes without compromising stretchability will favor to enhance the energy storage capacity. For metal–air batteries, doping with other elements to increase the activity of carbon materials for catalyzing oxygen redox reaction and oxygen evolution reaction rather than loading heavy catalyst is a promising method to improve the energy density.

Furthermore, it is challenging to compare reported stretchable energy storage devices' performances because of the lack of standard evaluation methods at present (Figure 8d). For one instance, specific capacitances on volume, area, or length are provided based on what the authors want to emphasize, and they may also be calculated from active materials, electrodes, or the entire device. For another instance, the stretchability is usually simply evaluated by tensile strains under stretching, but the body movements are comprehensive and sometimes irregular, so the evaluations on stretching property may fail to meet real wearable applications.

Overall, although stretchable energy storage devices have demonstrated attractive applications in wearable fields,

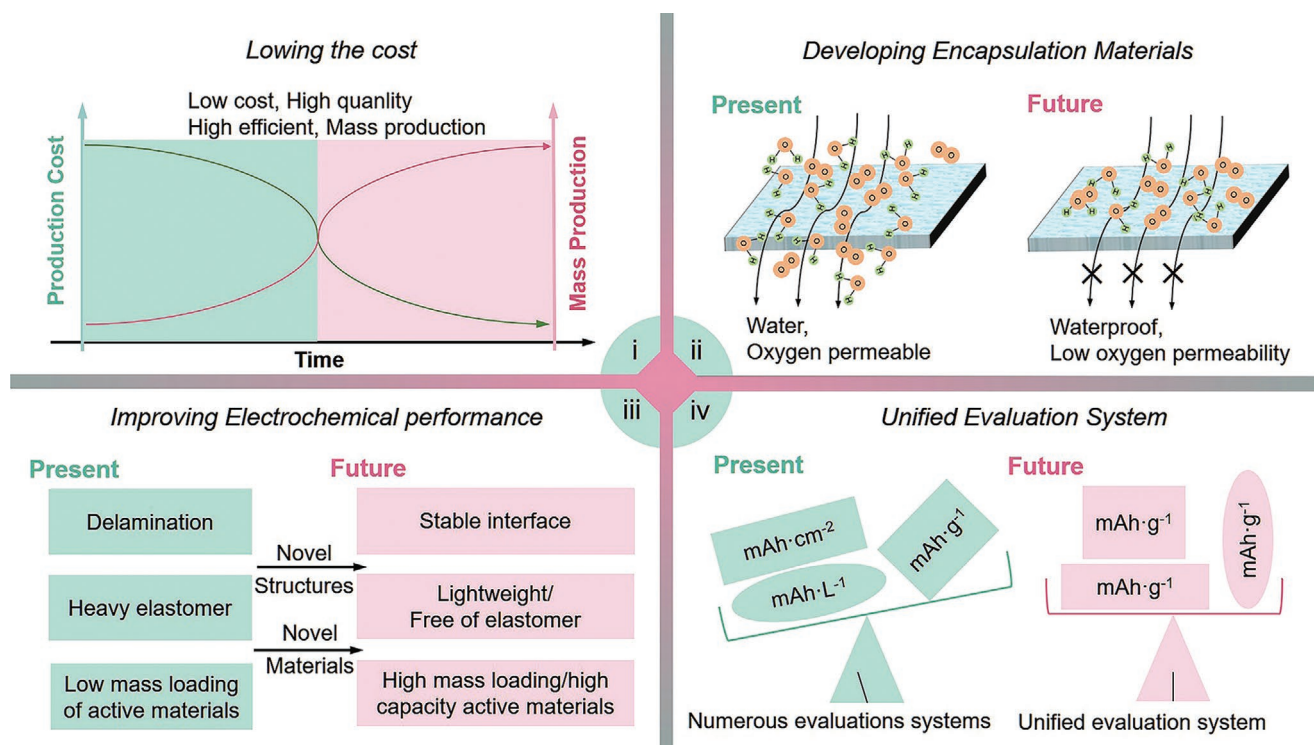


Figure 8. Challenges of carbon-material-based stretchable energy storage devices and their corresponding research directions.

they still face many challenges. As they involve a variety of research fields including chemistry, physics, materials science, electronics, and biomedical, it is critical to invite scientists from multidisciplinary fields to work together to solve the current problems. After decades of extensive studies, the stretchable energy storage devices may see real applications in wearable facilities, which undoubtedly enhance the life quality and change human beings' lifestyle in the future.

Acknowledgements

L.L. and L.W. contributed equally to this work. This work was supported by the Fundamental Research Funds for the Central Universities (Grant No. 021314380175), the Start-up Fund at Nanjing University (Grant No. 021314912221), and the National Postdoctoral Program for Innovative Talent (Grant No. BX20200161).

Conflict of Interest

The authors declare no conflict of interest.

Keywords

carbon materials, lithium-ion batteries, metal–air batteries, stretchable supercapacitors

Received: August 16, 2020
Revised: November 11, 2020
Published online:

- [1] S. Wang, J. Xu, W. Wang, G. Wang, R. Rastak, F. Molina-Lopez, J. W. Chung, S. Niu, V. R. Feig, J. Lopez, T. Lei, S. K. Kwon, Y. Kim, A. M. Foudeh, A. Ehrlich, A. Gasperini, Y. Yun, B. Murmann, J. B. Tok, Z. Bao, *Nature* **2018**, 555, 83.
- [2] Z. Wang, X. Guan, H. Huang, H. Wang, W. Lin, Z. Peng, *Adv. Funct. Mater.* **2019**, 29, 1807569.
- [3] C. Hou, Z. Xu, W. Qiu, R. Wu, Y. Wang, Q. Xu, X. Liu, W. Guo, *Small* **2019**, 15, 1805084.
- [4] J. Xu, S. Wang, G. N. Wang, C. Zhu, S. Luo, L. Jin, X. Gu, S. Chen, V. R. Feig, J. W. To, S. Rondeau-Gagne, J. Park, B. C. Schroeder, C. Lu, J. Y. Oh, Y. Wang, Y. H. Kim, H. Yan, R. Sinclair, D. Zhou, G. Xue, B. Murmann, C. Linder, W. Cai, J. B. Tok, J. W. Chung, Z. Bao, *Science* **2017**, 355, 59.
- [5] X. Chen, N. S. Villa, Y. Zhuang, L. Chen, T. Wang, Z. Li, T. Kong, *Adv. Energy Mater.* **2020**, 10, 1902769.
- [6] J. Kim, A. S. Campbell, B. E.-F. de Ávila, J. Wang, *Nat. Biotechnol.* **2019**, 37, 389.
- [7] L. Ma, Q. Liu, R. Wu, Z. Meng, A. Patil, R. Yu, Y. Yang, S. Zhu, X. Fan, C. Hou, Y. Li, W. Qiu, L. Huang, J. Wang, N. Lin, Y. Wan, J. Hu, X. Liu, *Small* **2020**, 16, 2000203.
- [8] L. Wang, X. Fu, J. He, X. Shi, T. Chen, P. Chen, B. Wang, H. Peng, *Adv. Mater.* **2020**, 32, 1901971.
- [9] L. Li, Z. Lou, D. Chen, K. Jiang, W. Han, G. Shen, *Small* **2018**, 14, 1702829.
- [10] J. Yang, J. Mun, S. Y. Kwon, S. Park, Z. Bao, S. Park, *Adv. Mater.* **2019**, 31, 1904765.
- [11] C. Cao, Y. Chu, Y. Zhou, C. Zhang, S. Qu, *Small* **2018**, 14, 1803976.
- [12] D. Chen, Z. Lou, K. Jiang, G. Shen, *Adv. Funct. Mater.* **2018**, 28, 1805596.
- [13] Q. Xue, J. Sun, Y. Huang, M. Zhu, Z. Pei, H. Li, Y. Wang, N. Li, H. Zhang, C. Zhi, *Small* **2017**, 13, 1701827.
- [14] Y. Zhou, C. Wang, W. Lu, L. Dai, *Adv. Mater.* **2020**, 32, 1902779.
- [15] D. Chen, K. Jiang, T. Huang, G. Shen, *Adv. Mater.* **2020**, 32, 1901806.

- [16] D. G. Mackanic, M. Kao, Z. Bao, *Adv. Energy Mater.* **2020**, *10*, 2001424.
- [17] L. Ye, Y. Hong, M. Liao, B. Wang, D. Wei, H. Peng, *Energy Storage Mater.* **2020**, *28*, 364.
- [18] H. Li, Y. Ding, H. Ha, Y. Shi, L. Peng, X. Zhang, C. J. Ellison, G. Yu, *Adv. Mater.* **2017**, *29*, 1700898.
- [19] C. Xia, J. Guo, Y. Lei, H. Liang, C. Zhao, H. N. Alshareef, *Adv. Mater.* **2018**, *30*, 1705580.
- [20] D. G. Mackanic, T. Chang, Z. Huang, Y. Cui, Z. Bao, *Chem. Soc. Rev.* **2020**, *49*, 4466.
- [21] W. Liu, M. Song, B. Kong, Y. Cui, *Adv. Mater.* **2017**, *29*, 1603436.
- [22] X. Zhang, H. Zhang, Z. Lin, M. Yu, X. Lu, Y. Tong, *Sci. China Mater.* **2016**, *59*, 475.
- [23] W. Ma, Z. Cai, Y. Zhang, Z. Wang, L. Xia, S. Ma, G. Li, Y. Huang, *Chin. J. Polym. Sci.* **2020**, *38*, 491.
- [24] X. Huang, X. Qi, F. Boey, H. Zhang, *Chem. Soc. Rev.* **2012**, *41*, 666.
- [25] X. Guo, S. Zheng, G. Zhang, X. Xiao, X. Li, Y. Xu, H. Xue, H. Pang, *Energy Storage Mater.* **2017**, *9*, 150.
- [26] S. Bae, H. Kim, Y. Lee, X. Xu, J.-S. Park, Y. Zheng, J. Balakrishnan, T. Lei, H. R. Kim, Y. I. Song, *Nat. Nanotechnol.* **2010**, *5*, 574.
- [27] L. Li, S. K. Hong, Y. Jo, M. Tian, C. Y. Woo, S. H. Kim, J. M. Kim, H. W. Lee, *ACS Appl. Mater. Interfaces* **2019**, *11*, 16223.
- [28] R. Raccichini, A. Varzi, S. Passerini, B. Scrosati, *Nat. Mater.* **2015**, *14*, 271.
- [29] Z. Li, J. Wang, S. Liu, X. Liu, S. Yang, *J. Power Sources* **2011**, *196*, 8160.
- [30] J. Yan, Z. Fan, T. Wei, W. Qian, M. Zhang, F. Wei, *Carbon* **2010**, *48*, 3825.
- [31] Q. Ke, C. Tang, Y. Liu, H. Liu, J. Wang, *Mater. Res. Express* **2014**, *1*, 025015.
- [32] Y. Shao, M. F. El-Kady, L. Wang, Q. Zhang, Y. Li, H. Wang, M. F. Mousavi, R. B. Kaner, *Chem. Soc. Rev.* **2015**, *44*, 3639.
- [33] J. Zang, C. Cao, Y. Feng, J. Liu, X. Zhao, *Sci. Rep.* **2014**, *4*, 6492.
- [34] H. A. Becerril, J. Mao, Z. Liu, R. M. Stoltenberg, Z. Bao, Y. Chen, *ACS Nano* **2008**, *2*, 463.
- [35] S. Gan, L. Zhong, T. Wu, D. Han, J. Zhang, J. Ulstrup, Q. Chi, L. Niu, *Adv. Mater.* **2012**, *24*, 3958.
- [36] D. Li, M. B. Muller, S. Gilje, R. B. Kaner, G. G. Wallace, *Nat. Nanotechnol.* **2008**, *3*, 101.
- [37] F. Gunes, H. J. Shin, C. Biswas, G. H. Han, E. S. Kim, S. J. Chae, J. Y. Choi, Y. H. Lee, *ACS Nano* **2010**, *4*, 4595.
- [38] Q. Ke, J. Wang, *J. Materiomics* **2016**, *2*, 37.
- [39] G. Wang, X. Sun, F. Lu, H. Sun, M. Yu, W. Jiang, C. Liu, J. Lian, *Small* **2012**, *8*, 452.
- [40] L. Qiu, X. Yang, X. Gou, W. Yang, Z. F. Ma, G. G. Wallace, D. Li, *Chem. - Eur. J.* **2010**, *16*, 10653.
- [41] Y. Si, E. T. Samulski, *Chem. Mater.* **2008**, *20*, 6792.
- [42] S. Li, Y. Luo, W. Lv, W. Yu, S. Wu, P. Hou, Q. Yang, Q. Meng, C. Liu, H. Cheng, *Adv. Energy Mater.* **2011**, *1*, 486.
- [43] G. Zhou, L. Li, C. Ma, S. Wang, Y. Shi, N. Koratkar, W. Ren, F. Li, H. Cheng, *Nano Energy* **2015**, *11*, 356.
- [44] J. Ren, R. Ren, Y. Lv, *Chem. Eng. J.* **2018**, *349*, 111.
- [45] B. Fang, D. Chang, Z. Xu, C. Gao, *Adv. Mater.* **2020**, *32*, 1902664.
- [46] Z. Xu, Y. Liu, X. Zhao, L. Peng, H. Sun, Y. Xu, X. Ren, C. Jin, P. Xu, M. Wang, C. Gao, *Adv. Mater.* **2016**, *28*, 6449.
- [47] Q. Zhang, J. Huang, W. Qian, Y. Zhang, F. Wei, *Small* **2013**, *9*, 1237.
- [48] T. W. Ebbesen, H. J. Lezec, H. Hiura, J. W. Bennett, H. F. Ghaemi, T. Thio, *Nature* **1996**, *382*, 54.
- [49] H. Li, H. Zhou, *Chem. Commun.* **2012**, *48*, 1201.
- [50] J. Ren, L. Li, C. Chen, X. Chen, Z. Cai, L. Qiu, Y. Wang, X. Zhu, H. Peng, *Adv. Mater.* **2013**, *25*, 1155.
- [51] Z. Niu, P. Luan, Q. Shao, H. Dong, J. Li, J. Chen, D. Zhao, L. Cai, W. Zhou, X. Chen, S. Xie, *Energy Environ. Sci.* **2012**, *5*, 8726.
- [52] Z. Yang, J. Tian, Z. Yin, C. Cui, W. Qian, F. Wei, *Carbon* **2019**, *141*, 467.
- [53] K. Liu, Y. Sun, L. Chen, C. Feng, X. Feng, K. Jiang, Y. Zhao, S. Fan, *Nano Lett.* **2008**, *8*, 700.
- [54] S. Iijima, *Nature* **1991**, *354*, 56.
- [55] J. E. Fischer, H. Dai, A. Thess, R. Lee, N. M. Hanjani, D. L. Dehaas, R. E. Smalley, *Phys. Rev. B* **1997**, *55*, R4921.
- [56] X. He, W. Gao, L. Xie, B. Li, Q. Zhang, S. Lei, J. M. Robinson, E. H. Házros, S. K. Doorn, W. Wang, *Nat. Nanotechnol.* **2016**, *11*, 633.
- [57] C. Preston, D. Song, J. Dai, Z. Tsinas, J. Bavier, J. Cumings, V. Ballarotto, L. Hu, *Nano Res.* **2015**, *8*, 2242.
- [58] K. Jiang, Q. Li, S. Fan, *Nature* **2002**, *419*, 801.
- [59] K. Liu, Y. Sun, P. Liu, X. Lin, S. Fan, K. Jiang, *Adv. Funct. Mater.* **2011**, *21*, 2721.
- [60] E. Oh, H. Cho, J. Kim, J. E. Kim, Y. Yi, J. Choi, H. Lee, Y. H. Im, K. H. Lee, W. J. Lee, *ACS Appl. Mater. Interfaces* **2020**, *12*, 13107.
- [61] X. Zhang, K. Jiang, C. Feng, P. Liu, L. Zhang, J. Kong, T. Zhang, Q. Li, S. Fan, *Adv. Mater.* **2006**, *18*, 1505.
- [62] W. Guo, C. Liu, X. Sun, Z. Yang, H. G. Kia, H. Peng, *J. Mater. Chem.* **2012**, *22*, 903.
- [63] T. Chen, Z. Cai, L. Qiu, H. Li, J. Ren, H. Lin, Z. Yang, X. Sun, H. Peng, *J. Mater. Chem. A* **2013**, *1*, 2211.
- [64] Y. Wei, K. Jiang, X. Feng, P. Liu, L. Liu, S. Fan, *Phys. Rev. B* **2007**, *76*, 045423.
- [65] Y. Zhang, W. Bai, J. Ren, W. Weng, H. Lin, Z. Zhang, H. Peng, *J. Mater. Chem. A* **2014**, *2*, 11054.
- [66] J. Yan, T. Wei, B. Shao, F. Ma, Z. Fan, M. Zhang, C. Zheng, Y. Shang, W. Qian, F. Wei, *Carbon* **2010**, *48*, 1731.
- [67] D. Wang, F. Li, Z. Chen, G. Q. Lu, H. Cheng, *Chem. Mater.* **2008**, *20*, 7195.
- [68] S. Prabakaran, R. Vimala, Z. Zainal, *J. Power Sources* **2006**, *161*, 730.
- [69] W. J. Song, J. Park, D. H. Kim, S. Bae, M. J. Kwak, M. Shin, S. Kim, S. Choi, J. H. Jang, T. J. Shin, S. Y. Kim, K. Seo, S. Park, *Adv. Energy Mater.* **2018**, *8*, 1702478.
- [70] J. Wei, D. Zhou, Z. Sun, Y. Deng, Y. Xia, D. Zhao, *Adv. Funct. Mater.* **2013**, *23*, 2322.
- [71] J. Wang, H. Liu, H. Sun, W. Hua, H. Wang, X. Liu, B. Wei, *Carbon* **2018**, *127*, 85.
- [72] H. Jiang, J. Ma, C. Li, *Adv. Mater.* **2012**, *24*, 4197.
- [73] T. Lin, I. Chen, F. Liu, C. Yang, H. Bi, F. Xu, F. Huang, *Science* **2015**, *350*, 1508.
- [74] X. Xie, T. Makaryan, M. Zhao, K. L. Van Aken, Y. Gogotsi, G. Wang, *Adv. Energy Mater.* **2016**, *6*, 1502161.
- [75] X. Xie, K. Kretschmer, J. Zhang, B. Sun, D. Su, G. Wang, *Nano Energy* **2015**, *13*, 208.
- [76] H. Jin, L. Zhou, C. L. Mak, H. Huang, W. M. Tang, H. L. W. Chan, *Nano Energy* **2015**, *11*, 662.
- [77] L. Gao, J. U. Surjadi, K. Cao, H. Zhang, P. Li, S. Xu, C. Jiang, J. Song, D. Sun, Y. Lu, *ACS Appl. Mater. Interfaces* **2017**, *9*, 5409.
- [78] A. Mishra, N. P. Shetti, S. Basu, K. Raghava Reddy, T. M. Aminabhavi, *ChemElectroChem* **2019**, *6*, 5771.
- [79] M. Cakici, R. R. Kakarla, F. Alonso-Marroquin, *Chem. Eng. J.* **2017**, *309*, 151.
- [80] D. C. Kim, H. J. Shim, W. Lee, J. H. Koo, D. H. Kim, *Adv. Mater.* **2020**, *32*, 1902743.
- [81] A. V. Korylyuk, P. van der Schoot, *Proc. Natl. Acad. Sci. USA* **2008**, *105*, 8221.
- [82] K. Y. Chun, Y. Oh, J. Rho, J. H. Ahn, Y. J. Kim, H. R. Choi, S. Baik, *Nat. Nanotechnol.* **2010**, *5*, 853.
- [83] F. Xu, Y. Zhu, *Adv. Mater.* **2012**, *24*, 5117.
- [84] T. Chen, H. Peng, M. Durstock, L. Dai, *Sci. Rep.* **2014**, *4*, 3612.
- [85] Y. Zhu, F. Xu, *Adv. Mater.* **2012**, *24*, 1073.
- [86] Q. Tang, M. Chen, G. Wang, H. Bao, P. Saha, *J. Power Sources* **2015**, *284*, 400.
- [87] W. Weng, Q. Sun, Y. Zhang, S. He, Q. Wu, J. Deng, X. Fang, G. Guan, J. Ren, H. Peng, *Adv. Mater.* **2015**, *27*, 1363.

- [88] Z. Xue, H. Song, J. A. Rogers, Y. Zhang, Y. Huang, *Adv. Mater.* **2019**, *32*, 1902254.
- [89] H. Jiang, Y. Sun, J. A. Rogers, Y. Huang, *Appl. Phys. Lett.* **2007**, *90*, 133119.
- [90] H. Jiang, Y. Sun, J. A. Rogers, Y. Huang, *Int. J. Solids Struct.* **2008**, *45*, 2014.
- [91] H. Jiang, D. Y. Khang, J. Song, Y. Sun, Y. Huang, J. A. Rogers, *Proc. Natl. Acad. Sci. USA* **2007**, *104*, 15607.
- [92] J. Song, H. Jiang, Z. J. Liu, D. Y. Khang, Y. Huang, J. A. Rogers, C. Lu, C. G. Koh, *Int. J. Solids Struct.* **2008**, *45*, 3107.
- [93] J. Yu, W. Lu, S. Pei, K. Gong, L. Wang, L. Meng, Y. Huang, J. P. Smith, K. S. Booksh, Q. Li, J. H. Byun, Y. Oh, Y. Yan, T. W. Chou, *ACS Nano* **2016**, *10*, 5204.
- [94] Y. Yu, Y. Luo, H. Wu, K. Jiang, Q. Li, S. Fan, J. Li, J. Wang, *Nanoscale* **2018**, *10*, 19972.
- [95] C. Cao, Y. Zhou, S. Ubnoske, J. Zang, Y. T. Cao, P. Henry, C. B. Parker, J. T. Glass, *Adv. Energy Mater.* **2019**, *9*, 1900618.
- [96] T. Chen, Y. Xue, A. K. Roy, L. Dai, *ACS Nano* **2014**, *8*, 1039.
- [97] Y. Z. Xie, Y. Liu, Y. Zhao, Y. H. Tsang, S. P. Lau, H. Huang, Y. Chai, *J. Mater. Chem. A* **2014**, *2*, 9142.
- [98] P. Xu, J. Kang, J. B. Choi, J. Suhr, J. Yu, F. Li, J. H. Byun, B. S. Kim, T. W. Chou, *ACS Nano* **2014**, *8*, 9437.
- [99] D. Qi, Z. Liu, Y. Liu, W. R. Leow, B. Zhu, H. Yang, J. Yu, W. Wang, H. Wang, S. Yin, X. Chen, *Adv. Mater.* **2015**, *27*, 5559.
- [100] D. Kim, G. Shin, Y. J. Kang, W. Kim, J. S. Ha, *ACS Nano* **2013**, *7*, 7975.
- [101] S. Xu, Y. Zhang, J. Cho, J. Lee, X. Huang, L. Jia, J. A. Fan, Y. Su, J. Su, H. Zhang, H. Cheng, B. Lu, C. Yu, C. Chuang, T. I. Kim, T. Song, K. Shigetani, S. Kang, C. Dagdeviren, I. Petrov, P. V. Braun, Y. Huang, U. Paik, J. A. Rogers, *Nat. Commun.* **2013**, *4*, 1543.
- [102] Y. Su, X. Ping, K. J. Yu, J. W. Lee, J. A. Fan, B. Wang, M. Li, R. Li, D. V. Harburg, Y. Huang, C. Yu, S. Mao, J. Shim, Q. Yang, P. Y. Lee, A. Armonas, K. J. Choi, Y. Yang, U. Paik, T. Chang, T. J. Dawidczyk, Y. Huang, S. Wang, J. A. Rogers, *Adv. Mater.* **2017**, *29*, 1604989.
- [103] Y. Zhang, H. Fu, S. Xu, J. A. Fan, K. C. Hwang, J. Jiang, J. A. Rogers, Y. Huang, *J. Mech. Phys. Solids* **2014**, *72*, 115.
- [104] Z. Song, X. Wang, C. Lv, Y. An, M. Liang, T. Ma, D. He, Y. Zheng, S. Huang, H. Yu, H. Jiang, *Sci. Rep.* **2015**, *5*, 10988.
- [105] Y. Morikawa, S. Yamagiwa, H. Sawahata, R. Numano, K. Koida, M. Ishida, T. Kawano, *Adv. Healthcare Mater.* **2018**, *7*, 1701100.
- [106] T. C. Shyu, P. F. Damasceno, P. M. Dodd, A. Lamoureux, L. Xu, M. Shlian, M. Shtein, S. C. Glotzer, N. A. Kotov, *Nat. Mater.* **2015**, *14*, 785.
- [107] R. Sun, S. C. Carreira, Y. Chen, C. Xiang, L. Xu, B. Zhang, M. Chen, I. Farrow, F. Scarpa, J. Rossiter, *Adv. Mater. Technol.* **2019**, *4*, 1900100.
- [108] S. Jiao, A. Zhou, M. Wu, H. Hu, *Adv. Sci.* **2019**, *6*, 1900529.
- [109] Z. Lv, Y. Luo, Y. Tang, J. Wei, Z. Zhu, X. Zhou, W. Li, Y. Zeng, W. Zhang, Y. Zhang, D. Qi, S. Pan, X. J. Loh, X. Chen, *Adv. Mater.* **2018**, *30*, 1704531.
- [110] Y. Zhang, W. Bai, X. Cheng, J. Ren, W. Weng, P. Chen, X. Fang, Z. Zhang, H. Peng, *Angew. Chem. Int. Ed.* **2014**, *53*, 14564.
- [111] P. Simon, Y. Gogotsi, *Nat. Mater.* **2008**, *7*, 845.
- [112] E. P. Gilshteyn, T. Kallio, P. Kanninen, E. O. Fedorovskaya, A. S. Anisimov, A. G. Nasibulin, *RSC Adv.* **2016**, *6*, 93915.
- [113] N. Li, G. Yang, Y. Sun, H. Song, H. Cui, G. Yang, C. Wang, *Nano Lett.* **2015**, *15*, 3195.
- [114] X. Wang, C. Yang, J. Jin, X. Li, Q. Cheng, G. Wang, *J. Mater. Chem. A* **2018**, *6*, 4432.
- [115] H. Li, T. Lv, H. Sun, G. Qian, N. Li, Y. Yao, T. Chen, *Nat. Commun.* **2019**, *10*, 536.
- [116] S. He, J. Cao, S. Xie, J. Deng, Q. Gao, L. Qiu, J. Zhang, L. Wang, Y. Hu, H. Peng, *J. Mater. Chem. A* **2016**, *4*, 10124.
- [117] C. Choi, S. H. Kim, H. J. Sim, J. A. Lee, A. Y. Choi, Y. T. Kim, X. Lepro, G. M. Spinks, R. H. Baughman, S. J. Kim, *Sci. Rep.* **2015**, *5*, 9387.
- [118] Z. Yang, J. Deng, X. Chen, J. Ren, H. Peng, *Angew. Chem. Int. Ed.* **2013**, *52*, 13453.
- [119] Z. Zhang, J. Deng, X. Li, Z. Yang, S. He, X. Chen, G. Guan, J. Ren, H. Peng, *Adv. Mater.* **2015**, *27*, 356.
- [120] G. Huang, C. Hou, Y. Shao, B. Zhu, B. Jia, H. Wang, Q. Zhang, Y. Li, *Nano Energy* **2015**, *12*, 26.
- [121] A. Lambertini, F. Clerici, M. Fontana, L. Scaltrito, *Adv. Energy Mater.* **2016**, *6*, 1600050.
- [122] Z. Zhang, L. Wang, Y. Li, Y. Wang, J. Zhang, G. Guan, Z. Pan, G. Zheng, H. Peng, *Adv. Energy Mater.* **2017**, *7*, 1601814.
- [123] T. Lv, Y. Yao, N. Li, T. Chen, *Angew. Chem. Int. Ed.* **2016**, *55*, 9191.
- [124] M. Yu, Y. Zhang, Y. Zeng, M. S. Balogun, K. Mai, Z. Zhang, X. Lu, Y. Tong, *Adv. Mater.* **2014**, *26*, 4724.
- [125] Q. Zhang, J. Sun, Z. Pan, J. Zhang, J. Zhao, X. Wang, C. Zhang, Y. Yao, W. Lu, Q. Li, Y. Zhang, Z. Zhang, *Nano Energy* **2017**, *39*, 219.
- [126] S. Wang, N. Liu, J. Su, L. Li, F. Long, Z. Zou, X. Jiang, Y. Gao, *ACS Nano* **2017**, *11*, 2066.
- [127] N. Li, T. Lv, Y. Yao, H. Li, K. Liu, T. Chen, *J. Mater. Chem. A* **2017**, *5*, 3267.
- [128] C. Choi, J. H. Kim, H. J. Sim, J. Di, R. H. Baughman, S. J. Kim, *Adv. Energy Mater.* **2016**, *7*, 1602021.
- [129] W. J. Song, S. Yoo, G. Song, S. Lee, M. Kong, J. Rim, U. Jeong, S. Park, *Batteries Supercaps* **2019**, *2*, 181.
- [130] W. Liu, Z. Chen, G. Zhou, Y. Sun, H. R. Lee, C. Liu, H. Yao, Z. Bao, Y. Cui, *Adv. Mater.* **2016**, *28*, 3578.
- [131] M. Gu, W. J. Song, J. Hong, S. Y. Kim, T. J. Shin, N. A. Kotov, S. Park, B. S. Kim, *Sci. Adv.* **2019**, *5*, eaaw1879.
- [132] X. Chen, H. Huang, L. Pan, T. Liu, M. Niederberger, *Adv. Mater.* **2019**, *31*, 1904648.
- [133] S. Kang, S. Y. Hong, N. Kim, J. Oh, M. Park, K. Y. Chung, S. S. Lee, J. Lee, J. G. Son, *ACS Nano* **2020**, *14*, 3660.
- [134] J. Ren, Y. Zhang, W. Bai, X. Chen, Z. Zhang, X. Fang, W. Weng, Y. Wang, H. Peng, *Angew. Chem., Int. Ed.* **2014**, *53*, 7864.
- [135] C. Li, Y. Sun, F. Gebert, S. L. Chou, *Adv. Energy Mater.* **2017**, *7*, 1700869.
- [136] L. Wang, Y. Zhang, J. Pan, H. Peng, *J. Mater. Chem. A* **2016**, *4*, 13419.
- [137] Y. Xu, Y. Zhang, Z. Guo, J. Ren, Y. Wang, H. Peng, *Angew. Chem. Int. Ed.* **2015**, *54*, 15390.
- [138] Y. Xu, Y. Zhao, J. Ren, Y. Zhang, H. Peng, *Angew. Chem. Int. Ed.* **2016**, *55*, 7979.
- [139] Y. Zhang, L. Wang, Z. Guo, Y. Xu, Y. Wang, H. Peng, *Angew. Chem. Int. Ed.* **2016**, *55*, 4487.
- [140] L. Ma, S. Chen, D. Wang, Q. Yang, F. Mo, G. Liang, N. Li, H. Zhang, J. A. Zapien, C. Zhi, *Adv. Energy Mater.* **2019**, *9*, 1803046.
- [141] Y. Wang, J. Liu, Y. Feng, N. Nie, M. Hu, J. Wang, G. Pan, J. Zhang, Y. Huang, *Chem. Commun.* **2020**, *56*, 4793.
- [142] S. Qu, Z. Song, J. Liu, Y. Li, Y. Kou, C. Ma, X. Han, Y. Deng, N. Zhao, W. Hu, C. Zhong, *Nano Energy* **2017**, *39*, 101.
- [143] Z. Shui, X. Liao, Y. Lei, J. Ni, Y. Liu, Y. Dan, W. Zhao, X. Chen, *Langmuir* **2020**, *36*, 12954.
- [144] S. Choi, D. Lee, G. Kim, Y. Y. Lee, B. Kim, J. Moon, W. Shim, *Adv. Funct. Mater.* **2017**, *27*, 1702244.
- [145] G. Liu, J. Y. Kim, M. Wang, J.-Y. Woo, L. Wang, D. Zou, J. K. Lee, *Adv. Energy Mater.* **2018**, *8*, 1703652.
- [146] L. Zhang, Y. Li, S. Zhang, X. Wang, X. Xia, D. Xie, C. Gu, J. Tu, *Small Methods* **2019**, *3*, 1900383.
- [147] W. Xu, C. Liu, Q. Wu, W. Xie, W.-Y. Kim, S.-Y. Lee, J. Gwon, *J. Mater. Chem. A* **2020**, *8*, 18327.
- [148] J. Liu, M. Hu, J. Wang, N. Nie, Y. Wang, Y. Wang, J. Zhang, Y. Huang, *Nano Energy* **2019**, *58*, 338.
- [149] Q. Zhang, J. Q. Huang, M. Q. Zhao, W. Z. Qian, F. Wei, *ChemSusChem* **2011**, *4*, 864.
- [150] L. Lin, H. Peng, Z. Liu, *Nat. Mater.* **2019**, *18*, 520.



Luhe Li is a Ph.D. candidate at the College of Engineering and Applied Sciences at the Nanjing University. He received his M.S. degree in 2019 from the Pusan National University, South Korea. His research focuses on the development of flexible energy storage devices, sensors, and their wearable applications.



Lie Wang is currently a postdoctoral scholar at the Nanjing University. He received his B.S. in Materials Science and Engineering from the Zhejiang Sci-Tech University in 2015 and his Ph.D. in Macromolecular Chemistry and Physics from the Fudan University in 2020. His research focuses on the development of flexible energy and electronic devices and their wearable applications.



Ye Zhang is currently an associate professor at the College of Engineering and Applied Sciences at the Nanjing University. She received her Ph.D. degree in Macromolecular Chemistry and Physics from the Fudan University in 2018 and then joined the Harvard Medical School as a postdoctoral research fellow. Her research focuses on the development of soft electronics including batteries, sensors, and bioelectronic devices.